Final Design Report
AME 40462 - Senior Aerospace Design
The Red Baron

Group #4:

"This is a Drag"

Alec Domotor
Claire Mariani
Connor Halloran
Harrison Yates
Steve Claucherty

May 6, 2015

Table of Contents

Conceptual Design

Design Proposal

Group #4 (“This is a Drag”) has been tasked with designing and constructing a new air taxi for Crazy Air Taxi Planes (CATplanes). CATplanes has asked for a fixed-wing aircraft that can accommodate two pounds of passengers, move these passengers quickly from place to place, and provide a thrilling experience by having high maneuverability. In response to these requests, the group decided to start making plans for a highly maneuverable biplane.

The biplane will be constructed using primarily balsa wood and lite plywood and reinforced with hardwood and carbon fiber. It will be powered by an E-flite Power 46 brushless motor and must carry at least five different types of passengers to meet the two pound requirement. The flight mission involves three laps unloaded and three laps loaded around the course. A lap is defined as two 500 ft straightaways with a 180 degree turn at each end and a 360 degree turn in the middle of one of the straightaways. The loaded and unloaded flights and the passenger loading time are combined to give a final mission time, so being able to quickly load the passengers is also an important consideration in the design.

Design Drivers

In this design, our main drivers came directly from the project assignment: speed, maneuverability, structural stability, and payload. To maximize the speed, the drag of the aircraft was minimized. At such a low scale, form drag will be a major source of drag and most of this will come from the fuselage, so this was a major concern during design. Unfortunately, the decision to make a biplane does increase the lift induced drag as well as the form drag on the wings, but we decided that the benefits outweighed the drawbacks. The maneuverability and structural stability were maximized through the implementation of a biplane design. Finally, the payload followed design constraints and involved the ability to carry 2 lbs of passengers and load/unload them quickly. Since this is the main requirement, this is the primary design driver.

Take-Off Weight Estimate

When estimating the takeoff weight, a few factors were already accurately known. From the project assignment, the non-expendable payload had to be at least 2 lbs. From material provided on the class website, the structure weight of the components given to us was 2.4 lbs. After this, estimations were used. For the structure weight of the fuselage besides the components given, the group estimated 1 lb. With the density of balsa wood around .004 lb/in^3, the structure would have to include 216 in^3 of wood in order to make this evaluation correct. The wing was also estimated at 1 lb based off of previous years' wing weights. Finally, an additional .4 lbs was calculated into the estimate as a 5% safety factor, in case any of the previous factors were greater than projected. All of these added up to a take-off weight of approximately 6.8 lbs.

Fuselage Design

The main design consideration for the fuselage was the payload requirement of the mission. The group decided on the following passenger configuration, working from the front of the cargo bay to the back: one Dolly, two Teds, two Lous, two Tater Tots (one under each Lou), and one Snoopy, for a total of two pounds. This means that the cargo bay section of the fuselage must be at least 9.5 inches long and a minimum of five inches wide at the front to accommodate Dolly's width. The passengers will all be flush with the top of the fuselage, and will be loaded from the back of the fuselage. Additionally, the passengers will be sitting in a Styrofoam tray that is cut to their specific dimensions. When we conduct the loading portion of the flight, this tray can easily be removed from the back of the fuselage, passengers placed into the tray, and then reloaded into the back of the fuselage.

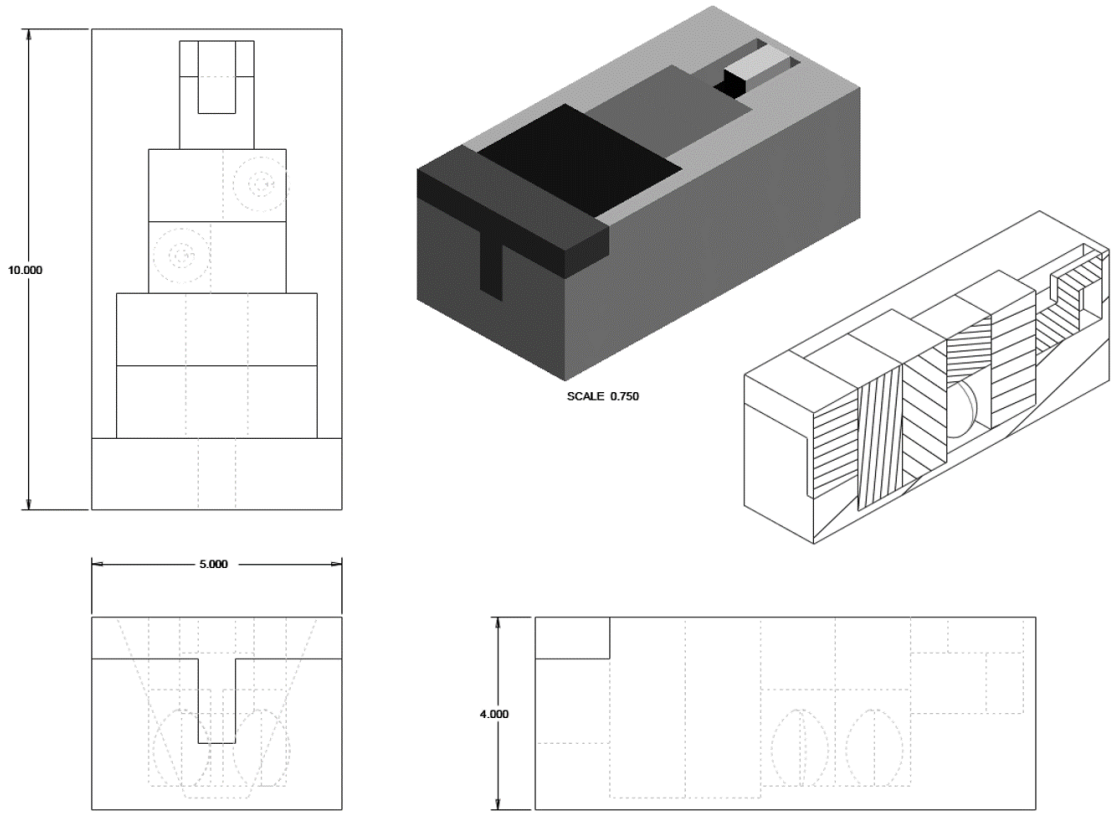

Figure 1: Passenger Set-Up

The nose of the plane will taper up from the bottom so that the motor is as close to the top of the aircraft as possible. This was done to allow for a fuselage with a lower height while still providing clearance for the propeller. The battery and controlling electronics will be located in the nose in front of the cargo area, to ensure stability and to keep the center of gravity relatively constant once the passengers are loaded. This provides a separation between the battery and controlling electronics and the payload, so the tray can be easily slid in and out without worrying about interfering with the electronics.

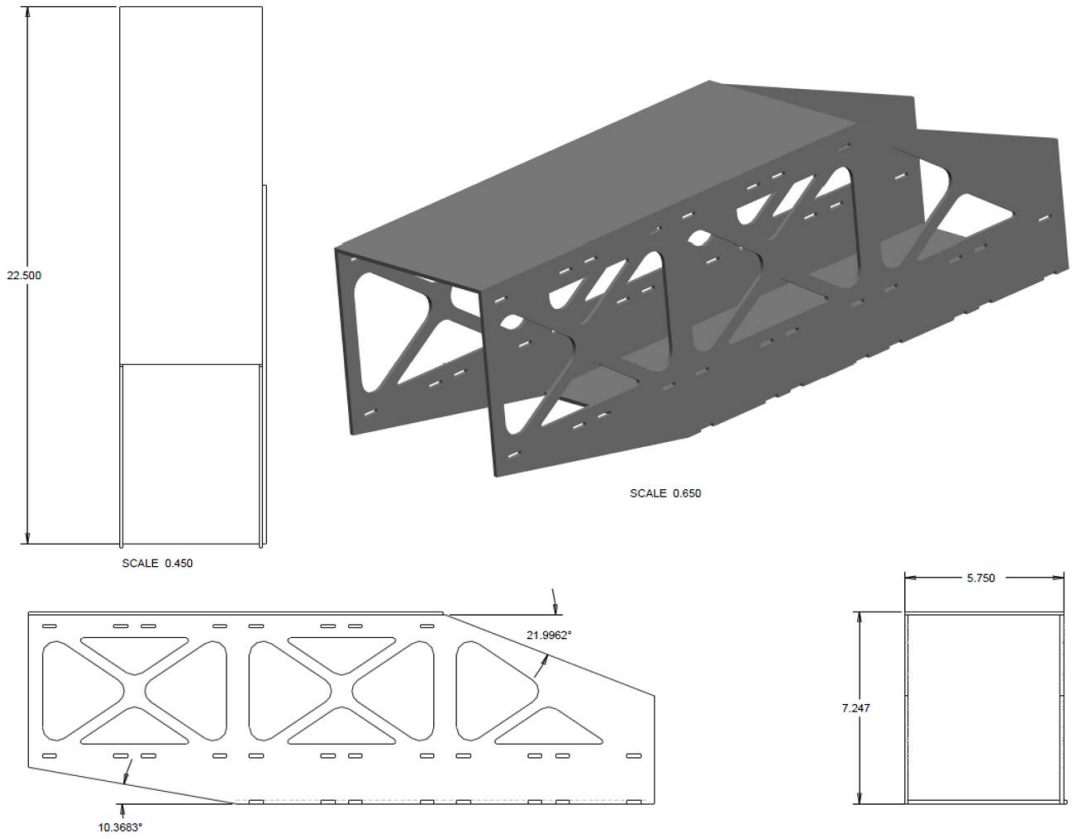

Figure 2: Fuselage Design

Wing Design

The group decided early on to go with a biplane. The main reason behind this was the increased maneuverability and reduced structure weight offered by the shorter wingspan of the biplane design. To get the lift required for level flight, the biplane requires a shorter wingspan and less area per wing than a monowing plane. However, the total wing area of the biplane will be greater than a monowing plane. This increased area will allow for a lower wing loading. The combination of a short wingspan and low wing loading should make the plane highly maneuverable.

Since the wings are shorter, the wings will require less structural support, and therefore less weight, to be robust. The biplane will require additional supportive struts between the wings, but the team decided that this increase in structure weight would be less than the weight savings from a shorter wing. Adding supportive struts will come at the cost of increased viscous drag, but lift-induced drag will dominate the total drag of the plane at this low velocity and Reynolds number, so it was not much of a concern.

A critical decision when trying to minimize the drag is the airfoil shape. The team selected the Clark-Y airfoil for multiple reasons. First, the Clark-Y is a very popular airfoil for general aviation and RC aircraft and appeared multiple times while researching low-Reynolds number airfoils. Second, the Clark-Y has a low thickness-to-chord ratio of 11.7%. This will decrease the drag produced by the wing. Finally, while in cruise, the aircraft will require a lift coefficient of .05. This falls within the drag bucket of the Clark-Y airfoil, which will produce a drag coefficient of ~0.04. An additional bonus of the Clark-Y airfoil is its flat lower surface, making it easy to construct and mount to the body of the plane.

For the final wing planforms, the upper and lower wings were chosen to have the same planform, with the upper wing staggered a half chord length in front of the bottom wing. Our research indicated that this positive stagger would improve the lift-to-drag characteristics of the wings. The individual wing areas were chosen to be 4.41 ft^2. This was based on the rule of

thumb that a biplane's effective wing area is equal to 150% of the area of one of its wings. For the best maneuverability, a low wing loading is necessary. This wing design will correspond to a wing loading of 1.03 lb/ft^2 when the aircraft is loaded with passengers, and 0.73 lb/ft^2 when unloaded.

A long chord length of 12.6 inches was selected to minimize the aspect ratio to achieve greater maneuverability. The wingspan came to 4.2 feet and the aspect ratio was calculated to be 4 per wing. A higher aspect ratio increases the sustained turn rate, so the aspect ratio of 4 was chosen to provide a balance between this and structural integrity. Traditionally, biplanes are constructed without taper, as it would have increased the already fairly large wingspan. The wing separation was decided upon to be 70% of the chord length and a positive stagger of 50% of the chord. While shorter than the optimal 1 chord length for each, it was the maximum distance we felt we could achieve with still maintaining structural stability. In this configuration, the airplane is estimated to have an instant turn rate of approximately 90 degrees per second, and a sustained turn rate of approximately 52 degrees per second, which means that the biplane would be able to complete the 360 degree turn in 7 seconds or less. This estimate assumes the plane will be flying at 55 ft/s.

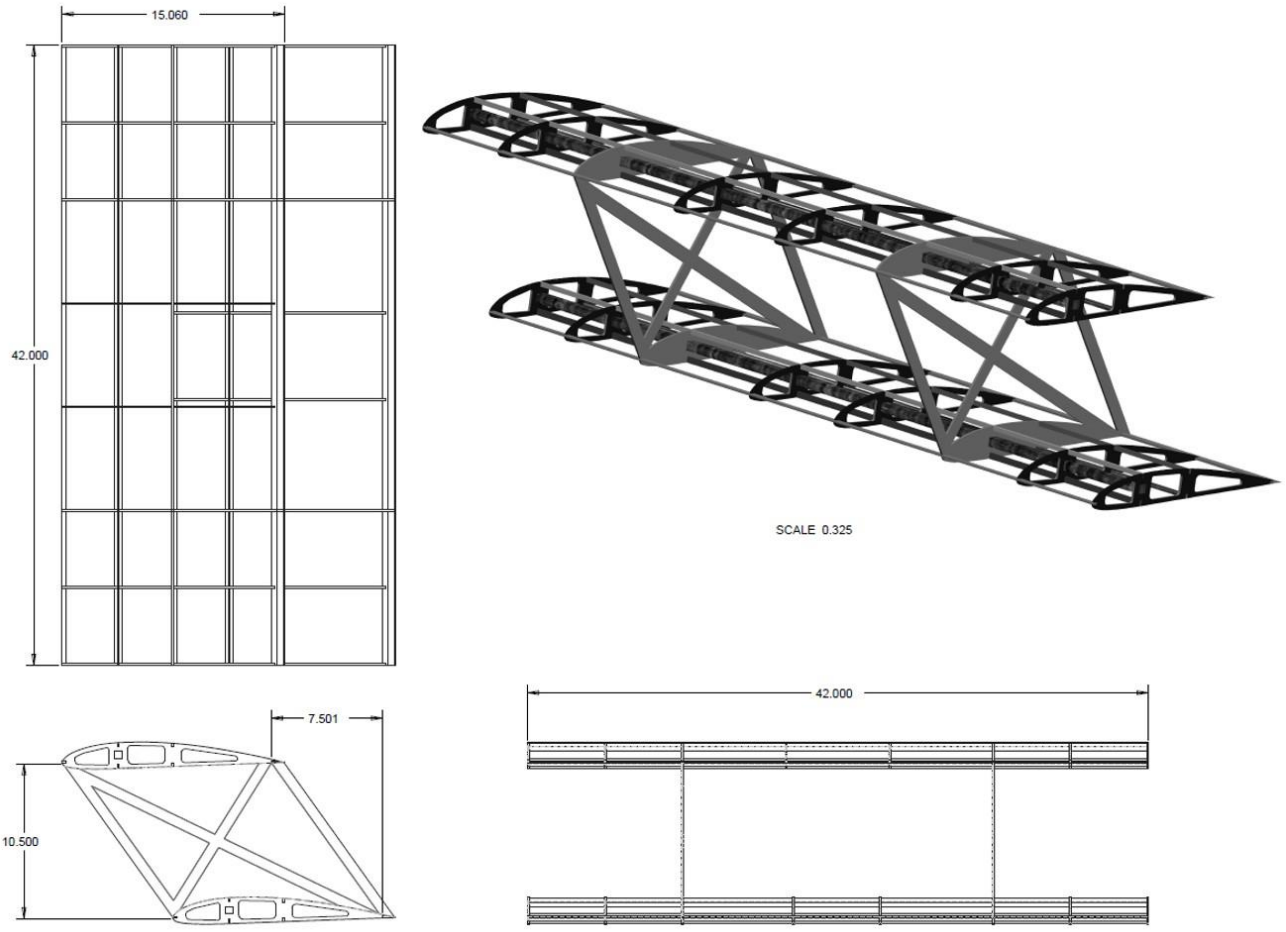

Figure 3: Wing Design

Tail Design

The tail of the airplane is going to be a triple boom tail. This will attach to the fuselage through the wing box at the bottom of the fuselage, and will extend approximately one foot aft of the fuselage. The three booms will be made of quarter inch square carbon fiber rods, and the tail surfaces will be flat balsa wood plates with no sweep or taper. From the center of lift of the mean aerodynamic chord (MAC) of the pair of main wings, which is located at approximately the leading edge of the bottom wing, a moment arm of two feet was used to size the tail. This provided the tail sizing parameters shown in Table 1. The control surfaces were sized based on the assumption that the ailerons need to be 20% of the effective area of the main wings, the rudder needs to be 30% of the vertical stabilizer, and the elevators need to be 25% of the area of the horizontal stabilizer.

Table 1. Tail surface sizes.

	b (ft)	c (ft)	AR	S (ft^2)
Horizontal Tail	2.15	.538	4	1.158
Vertical Tail	.75	.5	1.5	.37

Drag Analysis

When calculating the drag, the group used the spreadsheets from *Design of Aircraft* by Professor Corke, with some modifications made to accommodate this specific plane. The drag from the wing was calculated with the total wing area, not just the effective wing area. This returned a drag force of .1371 lbf. The fuselage was more difficult to estimate. The spreadsheets would only evaluate circular fuselage cross sections and the fuselage design was rectangular. Also, it was in the fuselage drag calculation that effect of the wing support structure unique to the biplane was accounted for. To account for this, the maximum distance on the rectangular cross section was used as the diameter in the spreadsheets. While an overestimation for the fuselage, this assumption was made to account for the support structure. In addition, the drag was then multiplied by 1.182, a correctional value from the article *Cutting Down the Drag*, in order to adjust for the rectangular shape. All of this resulted in a fuselage drag of .1623 lbf. The horizontal and vertical tail were both fairly standard, with the only difference being the use of flat plates. Both of these returned drag forces of .049 and .0105 lbf for the horizontal tail and vertical tail, respectively. All of the individual drags added together to produce a total drag of .3589 lbf. With an engine which has traditionally produced 3 lbf, this drag is well within the required limit. The results of the drag calculations are summarized in Table 2.

Table 2. Viscous Drag Forces by Component.

	Drag (lbf)	% Total
Fuselage	0.1623	45.22
Wing	0.1371	38.20
Hor. Tail	0.0490	13.65
Ver. Tail	0.0105	2.93
Total	0.3589	100.00

Stability

The stability for the aircraft was difficult to plan for, considering it had to be stable in two separate states. The first state accounted for was fully loaded with the passengers. The second state was unloaded. At this stage, the group could have used weight estimates from previous years to do stability calculations, but since the model of the plane was already created in CAD, a mass analysis was done in Creo 2.0. The individual parts were assigned the material properties of balsa wood, lite plywood, and Styrofoam, as was appropriate to the design. We then calculated the center of lift, which was found to be at the leading edge of the bottom wing. From this, the static margin, C_{M_alpha}, and C_{n_beta} were able to be calculated, and are shown in Table 3 for both the loaded and unloaded case.

Table 3. Static stability coefficients.

	Loaded	Unloaded
SM	0.0539	0.0347
C_{M_alpha}	-1.295	-1.236
C_{n_beta}	0.128	0.126

Conclusion and Future Considerations

Group 4 decided that the best way to meet the design parameters while still making a fast and maneuverable plane was to build a biplane. The group's plane utilizes a Clark Y airfoil configured in two wings, each with a span of 4.2 ft and a chord of 12.6 in, staggered by 50% of the chord length. The cargo bay is accessed through a hatch in the back of the fuselage roof, which allows for quick passenger loading. The configuration for the passengers is one Dolly, two Teds, two Lous, two Tater Tots (one under each Lou), and one Snoopy. Currently the empennage is set up as a triple boom tail with flat plane surfaces. Since the airplane is a tail dragger, the landing gear will be mounted in front of the bottom wing and to the rudder for directional control on the ground.

Moving forward in the design process, the group has identified some changes that may need to be made. The fuselage may be reduced slightly in size since it is larger than necessary to fit the passengers, but the additional length may be needed to support the wings. The control surfaces need to be resized to reflect the actual moment arm from the center of lift of the main wings to the center of lift of the tail surfaces, which means they will likely be smaller than in their current configuration. The group will also explore using a conventional tail instead of a boom tail to see if there is any real weight savings and if it makes sense structurally. The landing gear configuration and attachment needs to be finalized as does a battery mounting bracket. The parts in the assembly need to be checked to make sure they are the correct material and thickness and additional parts need to be created in CAD to complete the plane. The tail design will probably be the biggest issue going forward.

Performance Predictions

The performance predictions for the Red Baron are shown in Table 4.

Table 4. Performance predictions.

		Unloaded	Loaded
Minimum level speed	mph	17	20
Maximum level speed	mph	55	55
Maximum climb rate	ft/min	172	172
Best glide descent rate	ft/min	44	52
Best glide speed	ft/s	40	40
Maximum L/D	-	9.5	9.5
Load factor	-	4.3	2.9
Max instantaneous turn rate	deg/s	141.3	90.3
Max sustained turn rate	deg/s	65.5	52.4
Takeoff distance	ft	73	100
Landing distance	ft	96	123
Lap time	s	32	35

The maximum level speed was given to us by the pilots based on the motor and propeller combination that we are using. The minimum level speed was determined by the stall speed, which was calculated using Equation 1, where V_s is the stall velocity, W/S is the wing loading, ρ is the density of the air, and $C_{L,max}$ is the maximum lift coefficient.

$$V_s = \left[32.2 \frac{W}{S} \frac{2}{\rho C_{L,max}}\right]^{0.5} \quad (1)$$

The climb and descent rates were determined using Equations 2 and 3 with a climb and descent angle of 3 degrees, V is the airspeed, dH/dt is the climb/descent rate, ɣ is the climb/descent angle, and C_L is the lift coefficient with the minimum drag. The best glide speed was also an estimate based on talking to the pilots, who thought in our case it would be approximately two-thirds of our maximum level speed.

$$\frac{dH}{dt} = V\sin\gamma \tag{2}$$

$$\frac{dH}{dt} = \sin\gamma\sqrt{\frac{W}{S}\frac{2}{C_L/\cos\gamma}} \tag{3}$$

Our calculation of the maximum lift to drag ratio was based on the ratio of lift to lift induced drag of an equivalent single wing, so the value for our biplane is probably lower than this prediction due to added lift induced drag. The load factor is the ratio of the lift to the weight of the aircraft. The maximum instantaneous and sustained turn rates were determined using Equations 4 and 5, where phi dot is the turn rate, g is the gravitational parameter, n is the load factor, q is the dynamic pressure, A is the aspect ratio, e is Oswald's coefficient, T/W is the thrust to weight ratio, and $C_{D,0}$ is the drag coefficient at zero angle of attack.

$$\dot{\psi}_{max,i} = \frac{g\sqrt{n^2-1}}{V} \tag{4}$$

$$\dot{\psi}_{max,i} = \frac{g\sqrt{\frac{q\pi Ae}{W/S}\left[\left(\frac{T}{W}\right)_{max} - \frac{qC_{D,0}}{W/S}\right] - 1}}{V} \tag{5}$$

The takeoff and landing distances were computed using the methods outlined in *Design of Aircraft* by Corke, but neglecting the transition and climb elements for takeoff and the approach and transition elements for landing, as well as the safety factor of 1.6. The lap times were then determined using the velocity and turn rates calculated above.

Detailed Design

This section of the report gives a detailed overview of the final aircraft assembly and respective parts. Included in the appendix are detailed CAD part and assembly drawings in order to demonstrate the final design process. The aircraft design was altered in a few key areas following a design critique from the conceptual stage of the project.

Fuselage Changes

The fuselage design was changed in two key respects, the motivation behind this being to reduce form drag. As stated above, the fuselage computed to be the main source of viscous drag. The fuselage was made to be shorter and also have a smaller cross sectional area in order to improve this aspect of the design. Additionally, the divergence angle for the aft fuselage was altered to the angle limit (24°) recommended by Dr. Corke in Design of Aircraft. Beyond this limit, flow on the fuselage could separate. However, the group also wanted to reduced fuselage weight and overall profile, so this maximum angle was chosen in order to optimize all factors.

Tail Changes

Relative to the conceptual design, the detailed design provides a more robust boom and different vertical and horizontal tail stabilizer sizes. For the boom, the group had originally proposed using pre-made circular rods of 1/4'' in. diameter. However, upon evaluating these pieces, the group found them to be structurally insufficient. The group was particularly worried about torsional strength and flutter during flight. Therefore, a more robust design was made of a custom fabricated triangular boom. This piece was made of custom cut foam which provided several benefits. First, the new design could be increased to a significantly larger cross sectional area. This allowed the piece to be made as large as possible relative to the tail mounts. Also, the new material consisted of a carbon fiber and epoxy composite which provided more strength the pre-bought pieces could have. Additionally, a test piece of the new material was produced and found to be structurally sound for flight conditions.

The vertical and horizontal tail sizes were resized upon recommendations from the R/C pilots as well as Professors Corke and Juliano. The conceptual design contained stabilizers that were much too large for such an aircraft. The group had originally used the total main wing area of both the top and bottom wings in sizing the tail and control surfaces. In reality, this made the spreadsheet programs use a wing area that was much too large, as this computation only considers mono-wings. As a result, the group used a wing area equal to the total exposed area from a bird's eye view. This resulted in more reasonably sized stabilizers and control surfaces that will be shown in the detailed drawings section of the report. Finally, the tail mount used to connect the boom and tail components was slimmed down. The original design consisted of a circular disk that would have had a very high estimated drag coefficient of 1.3 (a flat plate perpendicular to the flow). The design was greatly improved by eliminating a majority of the surface area perpendicular to the flow while simultaneously increasing the surface area providing attachment points with the tail components.

Wing Changes

In general, the main wing design stayed the same in terms of planform dimensions, the airfoil, and other general geometric features. One main change involved the attachment point for the wing to the fuselage. The detailed design provides a large 1/4'' flat plate that was designed to bolt into the fuselage so that they would sit flush. The newly designed wing also offers more robustness as the ribs feature rounded external cutouts, spars were moved as per the recommendation of the pilots, and a flat plate was added to the attachment point for the ailerons.

Final Report

Flight Performance

Ground Mission

One might argue that the ground mission was the most successful of the mission stages for our group. The strategy of loading from the back with a hinged door covering the opening to prevent unnecessary drag worked very well. The best time recorded for the insertion of the passengers was 14.0 seconds, far and away the best time for any group. However, an overlooked part of the ground mission was battery insertion. Overlooked in the initial design stages, access to the electronics was dealt with after the fuselage had been fully constructed, but had yet to be monokoted. A very small door on the side of the fuselage was added to preserve structural integrity of the nose and was the only access to the electronics. This made putting in the battery very difficult. This stage of the ground mission took nearly as long as loading the passengers, at 12.1 seconds. These times resulted in a ground mission time of 26.1 seconds.

Flight 1: Mission 1 First Attempt

On the first attempt at the unloaded mission, the aircraft performed reasonably well. The aircraft finished the course in 1:50.2 and flew an average of 31.92 mph. At its fastest, the plane was able to travel 54.7 mph, while it only traveled 15.5 mph at its slowest. The plane was able to accelerate at a maximum of 115 feet per second squared. However, this occurred during a dive and only lasted for 0.1 second. As it was the first flight with the aircraft, turns were generally taken more gently, and only on the last lap was the strategy of climbing into and descending out of the turn practiced. Also, the pilot climbed for the first half of the flight, in order to have more recovery altitude, which cost time. Figure 4 gives an indication of the aircraft speed and flight path throughout flight attempt one.

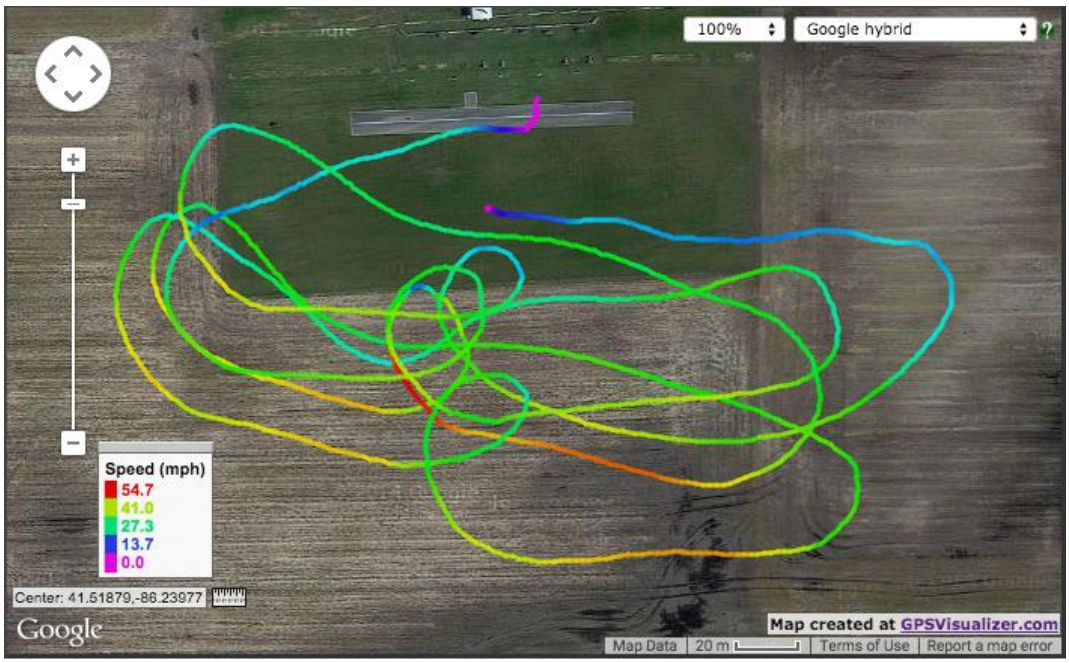

Figure 4. Flight attempt 1 (Mission 1) flight path with airspeed.

Flight 2: Mission 2 First Attempt

The team determined that it would be beneficial to complete both missions before attempting to improve flight scores from mission 1. Due to the designed loading configuration, the loaded plane had a center of gravity about 1/4'' ahead of the unloaded CG. This can be attributed to the fact that the payload was designed to be adjustable in the longitudinal direction. With this in mind, and also knowing that we had sufficient lift from mission one, mission two was attempted. First, it is important to note that as in the first flight attempt, the pilot had to adjust elevator pitch and obtain an overall feel for flying the plane loaded. Combined with battery issues as seen in flight attempt one, the team felt that flight attempts one and two did not see the aircraft realize its full performance potential.

As was expected with mission two, the aircraft flight performance was significantly affected by the presence of the additional payload. The aircraft completed the mission in 2:19.7. The team had predicted a loaded lap time of 34 seconds. This was based on the theoretical maximum airspeed, sustained turn rate, as well as the size of the course. The maximum speed the aircraft flew at was 44 mph, which did turn out to be significantly slower than flight attempt

one. From the flight data, the maximum level flight speed was found to be 41.7 mph, also a lower value. Figure 5 gives the flight attempt two flight path overlaid with the aircraft's speed throughout the flight. Additionally, it is worth noting that for this flight, GPS data is not available for the beginning of the flight. This can be visually seen in Figure 5, as the takeoff location via the runway is not visible.

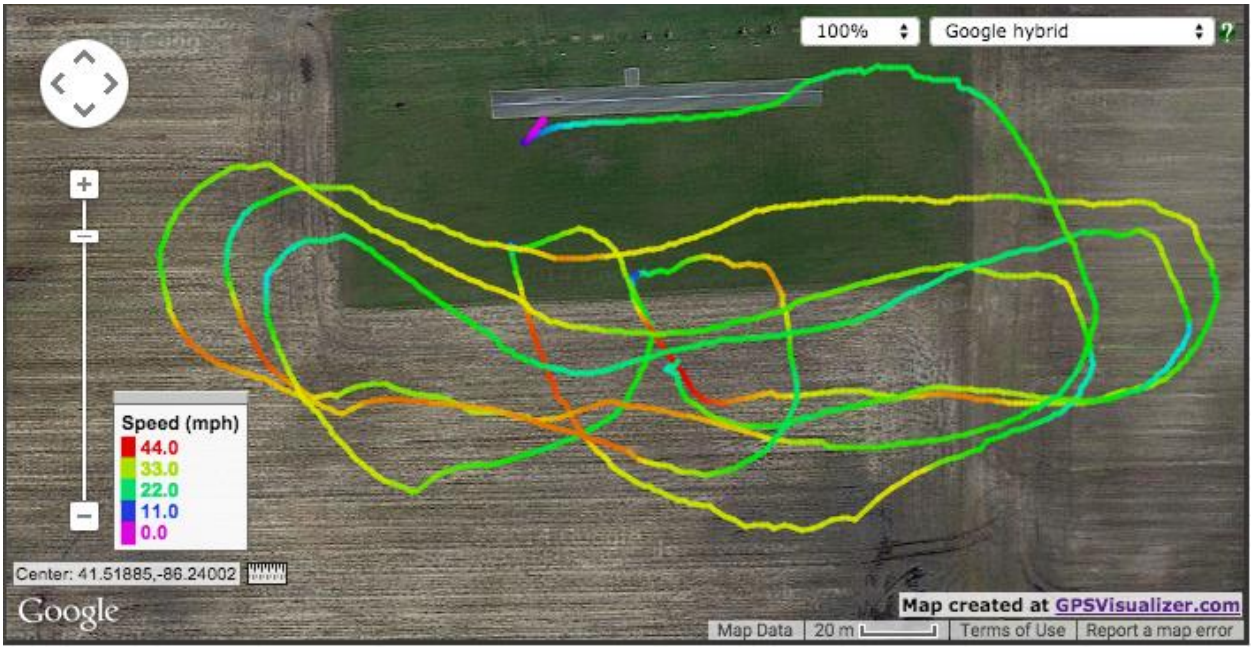

Figure 5. Flight attempt 2 (mission 2) flight path and airspeed.

Flight Attempt 3: Mission 1, Flight 2

This flight saw the team reattempt mission 1. There were several reasons for a new attempt. First, the team felt the aircraft did not reach its full potential on flight attempt 1. This was proved a valid point when this attempt saw the course completed in 128.4 seconds. The aircraft reached a maximum instantaneous speed of 51 mph exactly, based on GPS data. As was the case in previous flights, this was observed during a dive performed out of a turn. In flying the course, the pilot strategized to build altitude headed into the turn, and then use this to aid in building speed exiting the turn. This can be seen in two location in Figure 6, one occurring after the 180° turn on the west side of the course, and one occurring after the 360° turn. The

maximum sustained level flight speed of 46.8 mph was faster than the previous mission 1 attempt.

Improvements from flight attempt 1 included the use of a fully charged battery. Additionally, the pilot requested that the elevator be fixed to a more appropriate trim position for this flight. This meant fixing the neutral point of the elevator at an even higher deflection angle. However, this allowed the pilot to have more control over trim during flight (before the elevator had been at maximum trim during flight). This meant that while drag was added to the design, the pilot did not have to rely on motor thrust and finicky elevator controls to maintain level flight. While more drag was added, the higher level flight speed showed that adding more elevator trim was a good improvement to the design.

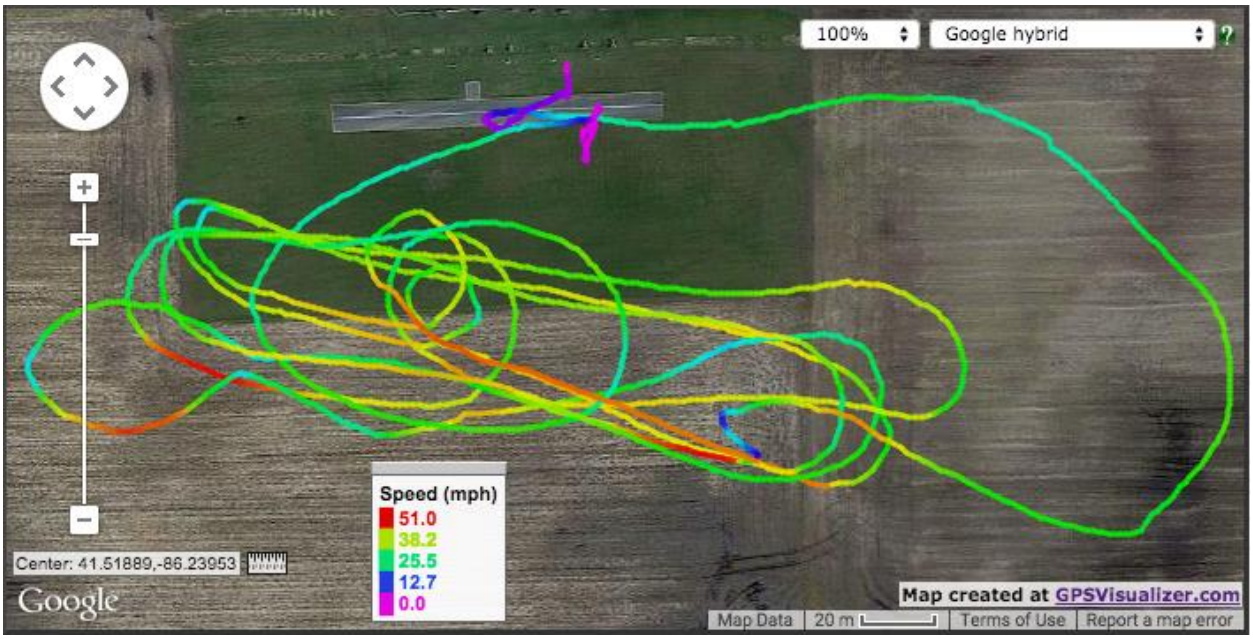

Figure 6. Flight attempt 3 (mission 1) flight path and airspeed.

Flight Attempt 4: Mission 2, Second Attempt

The final flight attempt for the group saw a second flight for the payload mission. As was the case with flight attempt 3, the group expected better overall performance due to the new elevator trimming as well as the use of a fully charged battery. The airplane reached a maximum of 45.6 mph, although this was in a dive out of the 360° turn. The maximum level

flight speed for the aircraft on this attempt was 40.2 mph. The team finished the mission in 152.6 seconds. This better time was reflected as a result of better aircraft performance. The average flight speed for this attempt was 20.71 mph.

Figure 7. Flight attempt 4 (mission 2) flight path and airspeed.

Final Results

For the unloaded flights, most of the best results were seen during the first flight, even though the time for the second flight was faster. We believe this occurred for two reasons. First, the aircraft began turning before hitting the edge of the field, which saved time on the turns. Second, the pilot climbed quite high before time began and was descending for a majority of the run, resulting in a faster average speed. This helped the overall time, but made certain statistics, such as level flight speed, invalid. This altitude management can be seen in Figure 8, discounting the last half of the second flight's altitude data, as aerobatics and not the mission were performed during this time.

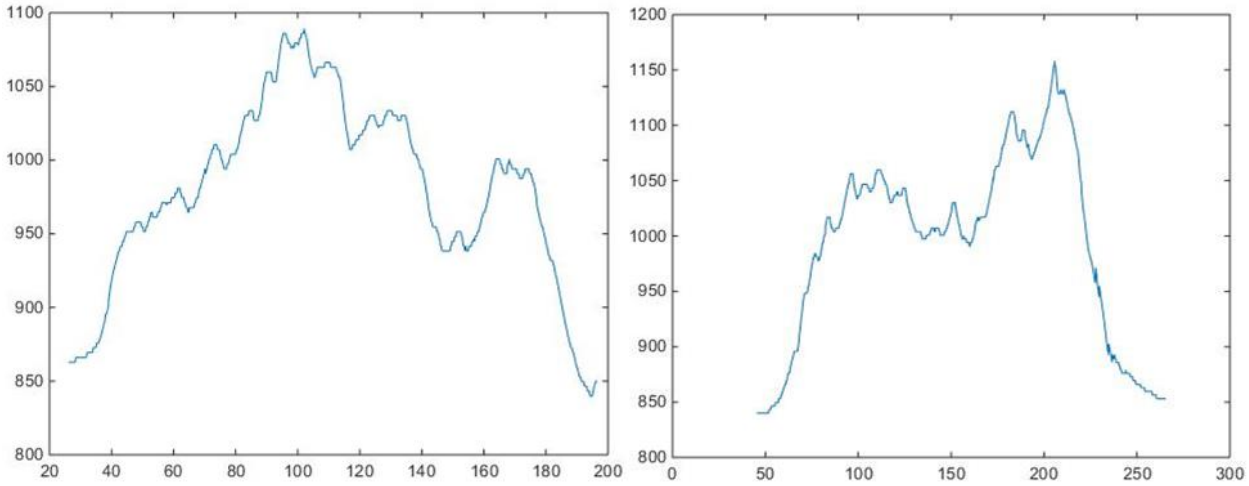

Figure 8. Altitude vs. Time in the First and Second Unloaded Mission Flights.

During flights without the payload, the highest level flight speed achieved was 41.78 mph and the lowest level flight speed was 32.19 mph. The maximum rate of climb achieved was 10.25 feet per second. The maximum rate of descent was 15.33 feet per second. The maximum sustained turn rate while at level flight was found to be 77.41 degrees per second. The maximum instantaneous turn rate during level flight was found to be 91.92 degrees per second. However, larger turn rates were achieved with velocity gained from dives, up to nearly 191 degrees per second when turning out of a dive.

From the pilot's estimation, he was able to bring the aircraft to a bank angle of 80 degrees during turns. This results in a load factor of approximately 5.75. The steepest gliding descent rate was 1.4729, traveling a distance of 9.5735 feet while descending 6.5 feet. This occurred during the landing approach. 1.4729 was also the maximum L/D ratio, which is quite low for monowing aircraft but fairly typical for biplanes. The maximum glide speed was 20.1 mph.

The minimum take off distance performed, when calculating from initial engine start up to overcoming a 35 foot obstacle, was 293.19 feet. This seems like an incredibly long distance, as the predicted distance is 4 times shorter, at 70 feet. However, this was due to the fact that, directly after liftoff, the pilot began to turn and did not begin the climb right away. The rolling and

rotating portion of takeoff was only ⅙ of the total take off distance, which came out to 50 feet. This implies that, if the aircraft tried to take off within the shortest distance, this distance could be reduced significantly. This shortest performed landing distance, using the 35 foot obstacle clearance again, was quite long as well, coming in at 210.93 feet. Here again, the rotating and rolling portion was a very small percentage of the total distance, coming to 38% of the total distance and 82.13 feet. This quite long, but a short landing distance was traded for the gentleness of the glide angle and glide time over the field to ensure a smooth landing.

During flights with the payload, the highest level flight speed achieved was 41.7 mph and the lowest level flight speed was 24.1 mph. The maximum rate of climb achieved was 17.5 feet per second. This is slightly higher than the max climb rate for the unloaded, but this may be due to the pilot becoming more comfortable with the aircraft after the first few runs. The maximum rate of descent was 7.36 feet per second. The maximum instantaneous velocity of 45.6 mph was achieved during a dive out of a 360° turn, as reflected in figure 4. The maximum sustained turn rate was computed to be 51.3°/s. This data was computed using GPS information from flight attempt 4, taking into account the aircraft heading values across various timesteps. Additionally, this turn took place during the final 360° turn, suggesting that the pilot felt more comfortable flying the loaded aircraft as the mission progressed. As can be seen from this parameter, the aircraft was not able to turn as quickly when loaded compared to the unloaded rate, also to be expected. Compared to a predicted maximum sustained turn rate of 52.4°/s from table 4, this value was within reason of the design specifications.

From video evidence, it appears that the airplane's loaded bank angle was about 60°. This leads to a load factor of 2 with the cargo. The glide descent rate was much higher for this landing at 4.0, traveling a distance of 26.4 feet while descending 6.6 feet. This suggests that it was not a true gliding descent and perhaps the pilot had more control over the plane during that particular descent.

The minimum take off distance performed, when calculating from initial engine startup to overcoming a 35 foot obstacle, was 253.44 feet. Like before, this was significantly higher than its predicted value, which loaded was at 100 ft. Again, the pilot took off right into a turn, so the calculated value is probably not as close as it could be. Due to the constraints of the airfield, immediately climbing straight up was not an option. The shortest performed landing distance was 285.12 feet, whereas the original approximation was at 123. This length in distance was worth it in the long run; this data comes from the final loaded flight, where the first attempt at landing was foiled by a random gust of wind that hit the plane about 10 feet off the ground. The pilot was able to quickly divert the landing, go around the pattern again, and then land smoothly with the minimum distance of 285.12 ft.

Discussion of Results

During testing, the first problem that became quite apparent right upon take off was the static instability. The plane displayed an odd flight pattern: it would first go nose up, almost stall, then go nose down, regain stability, and then the entire process would repeat for as long as the plane remained airborne. This very irregular flight pattern made it very difficult to control and predict, especially near the ground with no real altitude with which to recover. In addition, in order to maintain any degree of control, the pilot had to trim to full down elevator. This increased drag drastically and meant that there was no more control surface deflection if the aircraft needed to climb. This stability problem made the aircraft virtually unflyable and needed to be fixed before another flight was attempted.

The reason for the stability problem was not found to be the center of mass location, but rather in our prediction of the center of lift, as can be seen in Figure 9. The center of mass was where we had predicted, slightly forward of the leading edge of the bottom wing. However, the center of lift was nearly an inch forward of where we predicted it. The reason for incorrect prediction of the center of lift was the incline of the top wing. In the design of the wing, multiple sources described the advantages to having the top wing at a slightly higher angle of attack. Basically, the idea was to have the top wing stall first if the plane approached the stall angle of attack. This would send the center of lift aft, making the plane more nose heavy about the center of lift, leaving the plane easier to recover during a stall. In addition, the control surfaces were located on the bottom wing, so the stalling of the top wing would not affect control.

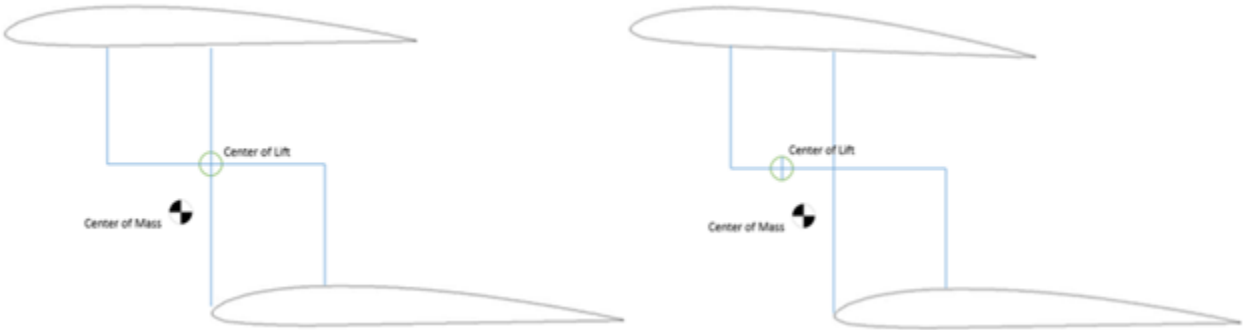

Figure 9. Predicted vs. Actual Center of Lift and Center of Gravity

A top wing at a higher angle of attack would also produce more lift at cruise. However, this proved to also have some negative effects as well. With the top wing producing more lift then it would if it was not at an angle of attack, the center of lift moved forward. Since the wings were staggered by half a chord length and assuming both wings produced the same lift, then the center of lift would be half way between the quarter chord points of the wings, which was at the leading edge of the bottom wing. While we believed that the 3 degree increase would not significantly affect the amount of lift produced, in practice, the top wing was producing 1.5 times the lift of the bottom wing at cruise. This meant, at no overall angle of attack, the center of lift was not at the leading edge of the bottom wing but rather 1.5 times closer to the quarter chord of the top wing than the bottom. This meant that the center of mass was aft of the center of lift.

This would also explain the odd flight pattern. The plane was tail heavy and would increase in angle of attack until stall. The top wing would stall first, producing no lift, while the bottom wing continued to produce lift. This would send the center of lift backward to the quarter chord of the bottom wing, behind the center of mass. This would make the plane stable and cause the nose to go down. This allowed the aircraft to recover, the front wing to regain flow, and the entire process to begin again.

In addition, we had a slight inclination problem between the wing's angle of attack and the horizontal stabilizers' angle of attack. Due to slight imperfections in construction of the tail, the horizontal stabilizers were at a slightly lower angle than the wing. This means that the stabilizers produced less lift at any angle of attack that the aircraft achieves than was estimated in the detailed design, as there was supposed to be no angle of attack change between the wing and the horizontal stabilizers. While this was not a large deflection, only 0.5 of a degree, this still reduced the center of lift by 0.02 at cruise. This moved the center of lift even further forward, compounding our problem.

If we were to design the aircraft again, a few changes would be made to mitigate this problem. First, the angle of attack of the top wing would be reduced to 2 or 1.5 degrees. This would provide all the advantages of the inclined top wing without having an overwhelming amount of lift. Second, the center of gravity would be moved forward by lighting some components aft of the center of lift. This could be done by holing out the underplate of the wing, which was two sheets of light ply glued together, and the rear of the fuselage, which did not support payload or other flight components. Third, the angle of attack of the horizontal stabilizers would be increased to even with the wing angle of attack, or even a slightly higher angle of attack. Finally, the center of lift was far easier to estimate for single wing aircraft, being at the quarter chord. Therefore, we would have considered this in the decision to make a biplane.

A second drawback to our aircraft was the large amount of drag it produced. This was made evident by the slow speed. While other groups were able to achieve maximum level speeds of over 50 feet per second, our aircraft was only able to travel at 41 feet per second. In addition, the maximum L/D was quite small. This did not come from a lack of lift, but rather an excess of drag. The high drag was a result of a few factors. First, the drag from biplanes is inherently larger than monowing aircraft. Planes with one wing typically have a coefficient of drag hovering around 0.02 to 0.025. Biplanes, on the other hand, have an expected drag coefficient of between 0.04 and 0.07. This can be seen in Figure 10, from the sharp decline in the lower bound in coefficients of drag was the biplane was replaced by the monoplane. Our aircraft had a drag coefficient of nearly 0.06, nearly double the coefficients of monowing groups. In addition, during the construction of our biplane, we opted to build a blunt trailing edge on both wings. This greatly improved the ease of construction and added strength by allowing us to run a stringer along the trailing edge, which made the wings easier to monokote. However, this created a less aerodynamic airfoil shape, and increased drag by creating flow separation. Also, the stability problems added drag, as the elevator was trimmed to 6 degrees of downward

deflection for level flight. This introduced more surface area into the flow at all times, producing more drag. Finally, the higher deflection of the top wing produces lift induced drag even while level. Lift induced drag dominates at such low speeds and this deflection produced this drag at cruise.

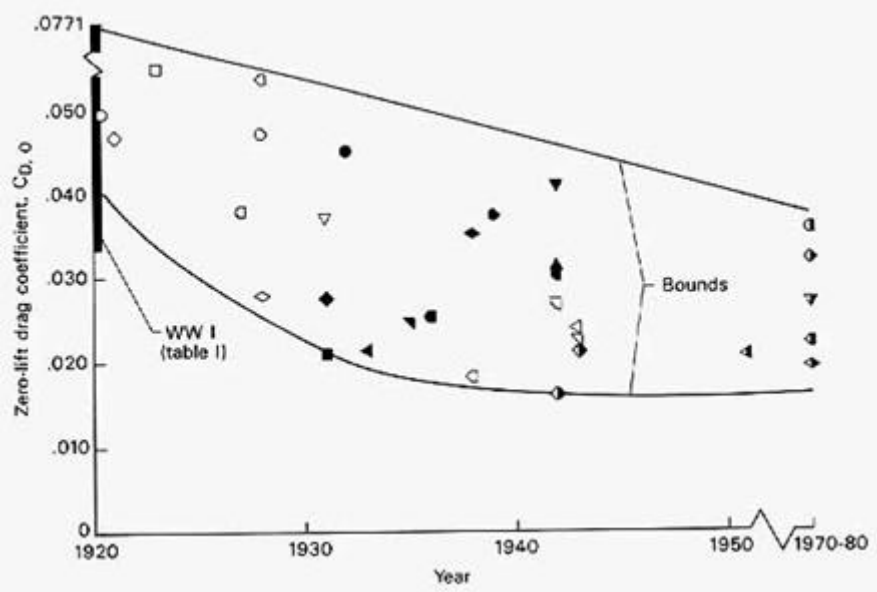

Figure 10. Upper and Lower Drag Coefficients over Time.

If we were to design the aircraft again, a few changes would have been made. First, wing rounds or winglets would be added to reduce the lift induced drag. By adding wing rounds, the efficiency factor of the wing increases, which will decrease the induced drag produced. Secondly, the center of gravity would be moved forward to fix the stability problem without the need for constant elevator deflection. Again, the deflection of the top wing would be reduced to a more reasonable level. Despite this, some of the drag problems are unavoidable. The biplane will always produces more drag than a monowing plane. The decision to build a biplane would more heavily consider the drag force. However, the benefits of the biplane still outweigh the costs.

The biplane also had numerous advantages, along with some of the inherent problems. First was the reason we selected the biplane, its superior maneuverability. Both the sustained

and instantaneous turn rates were very high, at 77.41 and 91.92 degrees per second respectively. However, much higher turn rates were achieved using velocity produced from a dive. This was possible because of the high bank angle, which was 80 degrees without the payload. This is incredibly steep and produced a large amount of stress on the aircraft. The places on the aircraft least equipped to deal with this are the wingtips, as these are basically the unsupported end of a cantilever. This leads to the second major advantage from the biplane, its natural structural strength.

With its use of two wings, a biplane can have the same wing area and wing loading as monowing planes with a much shorter wingspan. As the wing gets longer, the wingtip gets further and further away from the support offered by the fuselage. This means that the wing is weaker as the wingspan increases. In addition, the longer the wingspan, the greater the moment arm at the wing tip which the connection between the fuselage and the wing. Monoplanes can combat this with additional structure within the wing, but this adds weight. Biplanes, with their shorter wingspan, do not have this concern. This strength allows it to withstand much larger loads, as was witnessed by the bank angles achieved, as can be seen in Figure 7. At the impressive 80 degree bank angle, the load factor equaled 5.75, which means that force acting upon the aircraft is 5.75 times the usual force of gravity. Both major crashes which occurred on Tuesday occurred from wings breaking off during turns, when these high loads were applied. In order to avoid this, the short wingspans of the biplane was necessary.

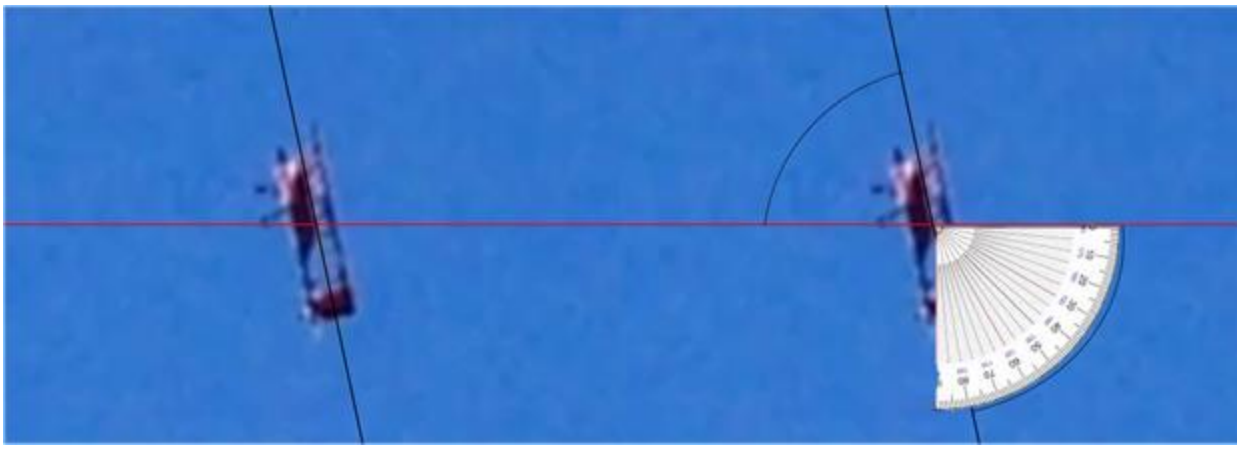

Figure 7. Bank Angle Unloaded

In addition, our aircraft also had a few design advantages which had nothing to do with a biplane. The first was the oversizing of control surfaces, especially the elevator. The elevator was nearly 20% of the horizontal stabilizer, which was quite large, especially compared to the other groups. Even the pilots questioned the size, suggesting a more tame number of 15%. However, the oversizing was necessary with the stability problems we experienced. The larger control surface gave the pilot more control, which he needed to keep the plane in the air. These control surfaces gave the plane superior survivability and recoverability. This could be seen in the third flight, in which the plane was able to recover from it full loop to level flight while only losing 23 feet in altitude from the top of the loop.

Appendix I

Conceptual Design Spreadsheets

Design Parameters				**Airfoil Data**				**Air Properties**		
M	0.05			Name	*Clark-Y*			Cruise Alt. (ft)	870	ft
S	4.38	ft2		Clmax	1.4			V	58.70	f/s
A	4.0			Cla	0.121	1/deg		ρ	0.074734178 26	lbm/f^3
ΛΛΕ	0	deg		a.c.	0.25	c		q	3.998615073	lbf/f^2
t/c	0.12			α0Λ	0	deg		μ	0.0000107	lbm/(f-s)
λ	1.00			Cd0	0.03			ν (χρυισε)	0.000143174 1172	f^2/s
W c-start	6.8	lbf/f^2		rle	0.0025	c				
W c-end	6.8	lbf/f^2		ClminD						
q c-start	4.00	lbf/f^2		(t/c)max	0.20	c				
q c-end	4.00	lbf/f^2								
Cl c-start	0.39									
Cl c-end	0.39									
Calculations				**Sweep Angles**						
b	4.2	ft			x/c	Λξ/χ (δεγ)				
Meff	0.05			LE	0.00	0.0				
cr	1.05	ft		1/4C	0.25	0.0				
ct	1.05	ft		a.c	0.25	0.0				
m.a.c.	**1.0**	ft		(t/c)max	0.20	0.0				
				TE	1.00	0.0				
β	1.00									
CLa	**0.068**	1/deg		**Viscous Drag**						
CLo	0.00			V_eff	58.7	f/s				
ατριμ	**5.7**	deg		q_eff	3.998615073	lbf/f^2				
CLtrim	0.388			Re_mac	4.29E+05					
k	0.099471 83943			sqrt(Re)	654.9985271					
CD	**0.019**			Cf	2.03E-03					
L/D	**20.00**			S_wet	8.9257392	ft2				

				F	1.070427308				
				Q	1				
Total Drag	**0.3399005213**	lbf		CD0	**0.004422674876**				
Spanwise View									
x	y								
0	0								
1.0	0								
1.05	2.092844954								
0	2.092844954								
0	0								
Lift Curves									
α	Cl	α	CL						
0	0	0	0						
11.57024793	1.4	11.57024793	0.784716176						

Wing design.

Take-off			**Landing**	
H (f)	899		H (f)	899
CL(max)	1.6		CL(max)	1.6
T(max) (lb)	3		T(max) (lb)	3
W_TO (lb)	6.8		W_L (lb)	6.8
S (f^2)	6.62		W/S (lb/f^2)	1.027966742
W/S (lb/f^2)	1.027966742		S (f^2)	6.615
SIGMA	0.97649115		SIGMA	0.97649115
T/W	0.4411764706		T/W	0.4411764706
TOP	1.491346049		LP	0.6579467862
S_TO (f)	101.738242		S_TO (f)	477.6377208
Cruise Start			**Cruise End**	
CD_0	0.004		CD_0	0.004
A	4.5		A	4.5
H (f)	899		H (f)	899
Cruise Mach	0.05		Cruise Mach	0.05
W (lb)	4.8		W (lb)	5
k	0.08841941283		k	0.08841941283
V (f/s)	55.04717		V (f/s)	55.04717
rho (lbm/f^3)	0.07467618421		rho (lbm/f^3)	0.07467618421
q (lbf/f^2)	3.513712666		q (lbf/f^2)	3.513712666
W/S (lb/f^2)	0.5284542911		W/S_optimum	0.5284542911
S (f^2)	6.615		W/S_actual	0.7256235828
Climb			**Acceleration**	
H (f)	0		H (f)	10,000
Climb Mach	0.05		Cruise Mach	0.05
dH/dt (f/min)	900		n	1.7
V (f/s)	55.2			
G (rad)	0.2717391304		V (f/s)	53.5
Gamma (deg)	15.76778149		rho (lbm/f^3)	0.056476049
rho (lbm/f^3)	0.076474		q (lbf/f^2)	2.510070982
q (lbf/f^2)	3.618312686		W/S (lb/f^2)	0.3140459985
T/W min	0.309			
T/W min - G	0.038			
W/S_+ (lb/f^2)	0.7695951006			
W/S_- (lb/f^2)	0.7695950403			
Turn - Inst.			**Turn- Sustained**	
H (f)	899		H (f)	899

Cruise Mach	0.05		Cruise Mach	0.05
CL_max	0.9		n	2.87
W/S (lb/f^2)	1.1		W/S (lb/f^2)	1.1
V (f/s)	55.04717		T/W_max	0.1079482737
rho (lbm/f^3)	0.07467618421		V (f/s)	55.04717
q (lbf/f^2)	3.513712666		rho (lbm/f^3)	0.07467618421
psi_dot (rad/s)	1.576640165		q (lbf/f^2)	3.513712666
psi_dot (deg/s)	90.33490357		psi_dot (rad/s)	0.9133885768
n	2.874855818		psi_dot (deg/s)	52.33335471
Ceiling			**Decent**	
W (lb)	4.8		W (lb)	6.8
S (f^2)	6.615		S (f^2)	6.615
H (f)	1,000		H (f)	899
Cruise Mach	0.05		Cruise Mach	0.05
W/S (lb/f^2)	0.7256235828		W/S (lb/f^2)	1.027966742
V (f/s)	55.03		V (f/s)	55.04717
rho (lbm/f^3)	0.0744742049		rho (lbm/f^3)	0.07467618421
q (lbf/f^2)	3.502023319		q (lbf/f^2)	3.513712666
CL_required	0.2072012425		dH/dt-min (f/min)	168.235537
			Gamma (deg)	2.91972604

Takeoff and Landing Distances.

Flight Regime Data:								
Cruise Mach	0.05							
Cruise Alt. (ft)	899							
V (f/s)	55.05							
ρ (λβμ/ϕ⊥3)	0.074676							
q (lbf/f^2)	3.513712							
μ (λβμ/(ϕ−σ))	0.000010							
ν (χρυισε) (ϕ⊥2/σ)	0.000143							
Dimension Data:			**Form Factors:**					
D-max (ft)	0.7708333333		*F*	1.292777778				
L/D	6		*Q*	1				
L (ft)	4.6250		*F*Q*	1.292777778				
S (f^2)	6							
Viscous Drag Calculations:			*Cone-Cylinder Fuselage Shape*					
x/L	x (ft)	x-L/4 (ft)	D (ft)	P (ft)	Sw(ft^2)	Rex	CF	Drag (lbf)
0.00	0.00	-1.16	0	0.0				
0.10	0.46	-0.69	0.3854166667	1.2	0.6	1.8E+05	3.15E-03	0.008014155
0.20	0.93	-0.23	0.7708333333	2.4	1.1	3.6E+05	2.23E-03	0.011333727
0.30	1.39	0.23	0.7708333333	2.4	1.1	5.3E+05	1.82E-03	0.009253950
0.40	1.85	0.69	0.7708333333	2.4	1.1	7.1E+05	1.58E-03	0.008014155
0.50	2.31	1.16	0.7708333333	2.4	1.1	8.9E+05	1.41E-03	0.007168079
0.60	2.78	-	0.7708333333	2.4	1.1	1.1E+06	4.42E-03	0.022470508
0.70	3.24	-	0.7708333333	2.4	1.1	1.2E+06	4.29E-03	0.021839217
0.80	3.70	-	0.7708333333	2.4	1.1	1.4E+06	4.19E-03	0.021312089
0.90	4.16	-	0.3854166667	1.2	0.6	1.6E+06	4.10E-03	0.010430836
1	4.63	-	0	0.0	0.0	1.8E+06	4.02E-03	0.000000000
Totals:					**9.0**			**0.119836716**
Total Drag:	**0.1198367**	**lbf**						
Equiv. CD	0.005622486335							

Fuselage Design.

Main Wing Reference				**Air Properties**				
b	4.2	ft	Cruise Alt. (ft)	899	ft			
m.a.c.	1.4	ft	V	55.05	f/s			
S	6.57	ft2	ρ	0.0746761842 1	lbm/f^3			
M	0.05		q	3.513712666	lbf/f^2			
ΛΛΕ	0	deg	μ	0.0000107	lbm/(f-s)			
t/c	0.12		ν (χρυισε)	0.0001432853 073	f^2/s			
λ	1.00							
Vertical Tail								
Design Parameters			**Airfoil Data**					
Cvt	*0.03*		Name	*NACA 64-004*				
Lvt	*2.0*	ft	Clmax	*0.97*				
ΛΛΕ	*0*	deg	Cla	*0.097*	1/deg			
t/c	*0.02*		a.c.	*0.25*	c			
λ	*1.00*		α0Λ	*0*	deg			
Avt	*1.50*		Cd	*0.027*				
Calculations			**Sweep Angles**			**Viscous Drag**		
Svt	0.6026	ft2		x/c	Λξ/χ (δ εγ)	V_eff	55.04717	f/s
b	1.0	ft	LE	0.00	0.0	q_eff	3.513712666	lbf/f^2
cr	0.6	ft	1/4 chord	0.25	0.0	M_eff	0.05	
ct	0.6	ft	(t/c)max	0.50	0.0	Re_mac	243684.5801	
m.a.c.	0.6	ft	TE	1.00	0.0	sqrt(Re)	493.6441836	
β	1.00					Cf	2.69E-03	
CLa	**0.037**	1/deg				S_wet	1.2070078	ft2
						F	0.8765547883	
						Q	1.05	
Total Drag	**0.010501**	lbf				CD0	**4.96E-03**	

Spanwise View

x	y
0	0
0.6	0
0.6	1.0
0	1.0
0	0

Horizontal Tail								
Design Parameters			**Airfoil Data**					
Cht	0.60		Name	*NACA 64-004*				
Lht	1.9		Clmax	*0.8*				
ΛΛΕ	0	deg	Cla	*0.111*	1/deg			
t/c	0.14		a.c.	*0.258*	c			
λ	1.00		α0Λ	*0*	deg			
Aht	3.00		Cd	*0.004*				
Calculations			**Sweep Angles**			**Viscous Drag**		
Sht	2.55	ft2		x/c	Λξ/χ (δ εγ)	V_eff	55.04717	f/s
b	2.8	ft	LE	0.00	0.0	q_eff	3.513712666	lbf/f^2
cr	0.8	ft	1/4 chord	0.25	0.0	M_eff	0.05	
ct	0.8	ft	(t/c)max	0.50	0.0	Re_mac	299659.4237	
m.a.c.	0.8	ft	TE	1.00	0.0	sqrt(Re)	547.411567	
β	1.00					Cf	2.43E-03	
CLa	**0.059**	1/deg				S_wet	5.22699	ft2
						F	1.03707263	
						Q	1.05	
Total Drag	**0.049**	lbf				CD0	**0.005414945197**	

Spanwise View

x	y
0	0
0.8	0
0.8	1.4
0	1.4
0	0

Tail Surface Design.

Appendix II

Detailed Design CAD

Figure 1. Complete Assembly Front.

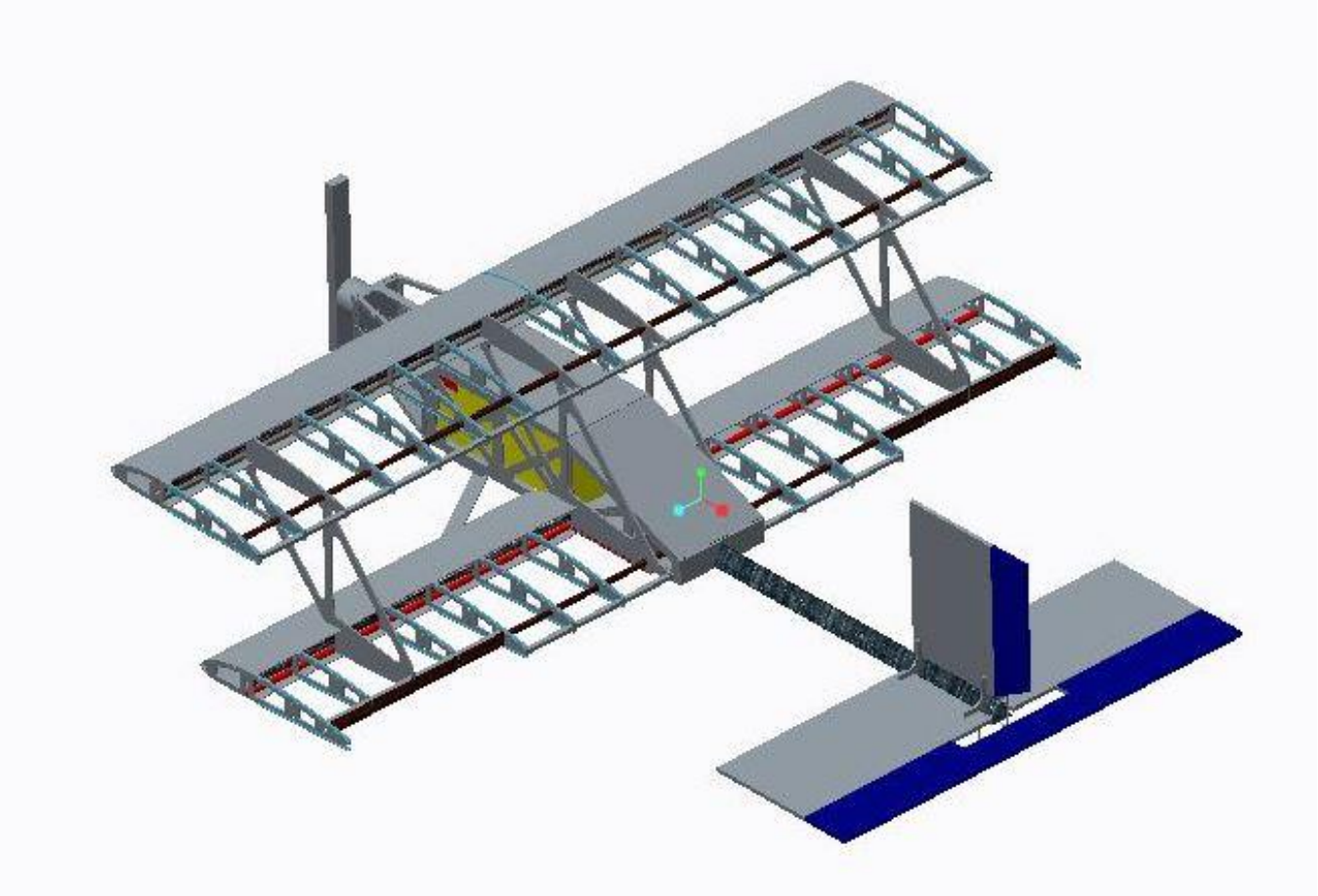

Figure 2. Complete Assembly Rear.

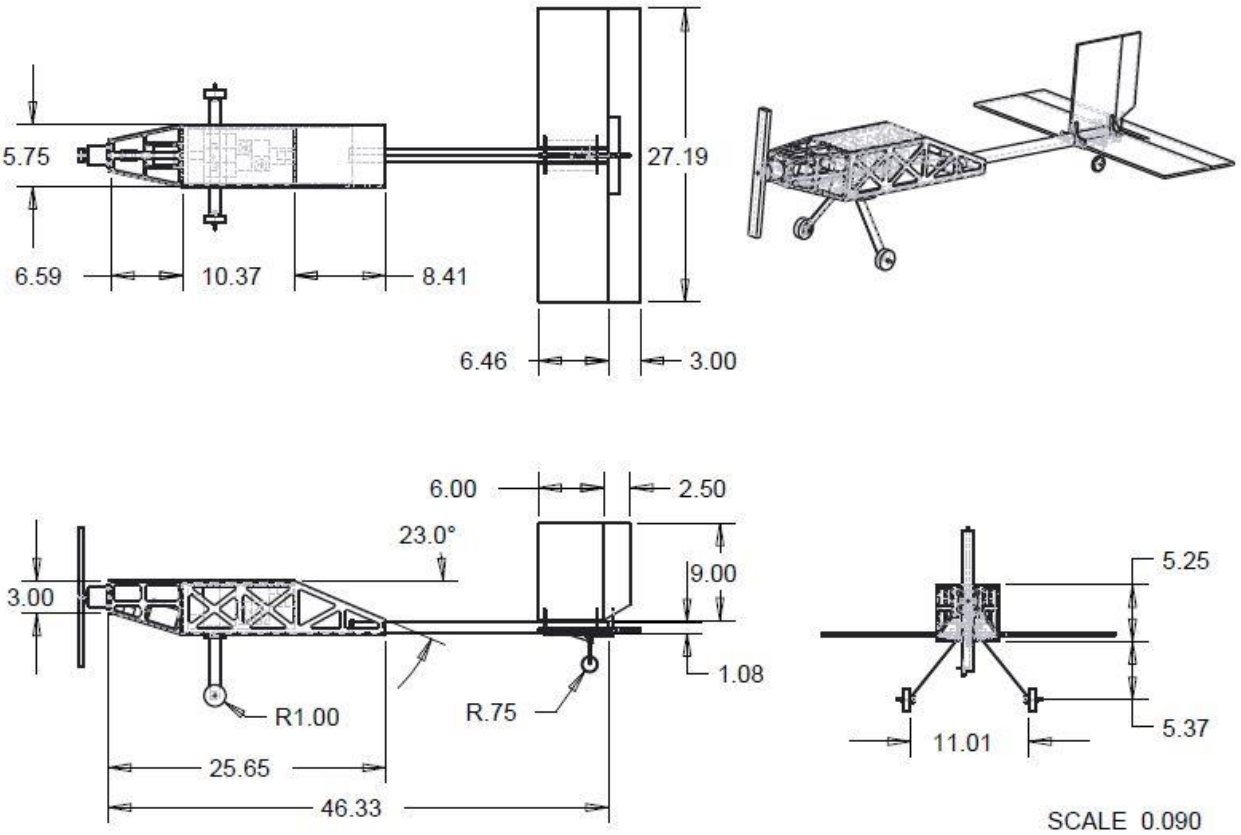

Figure 3. Fuselage Detailed.

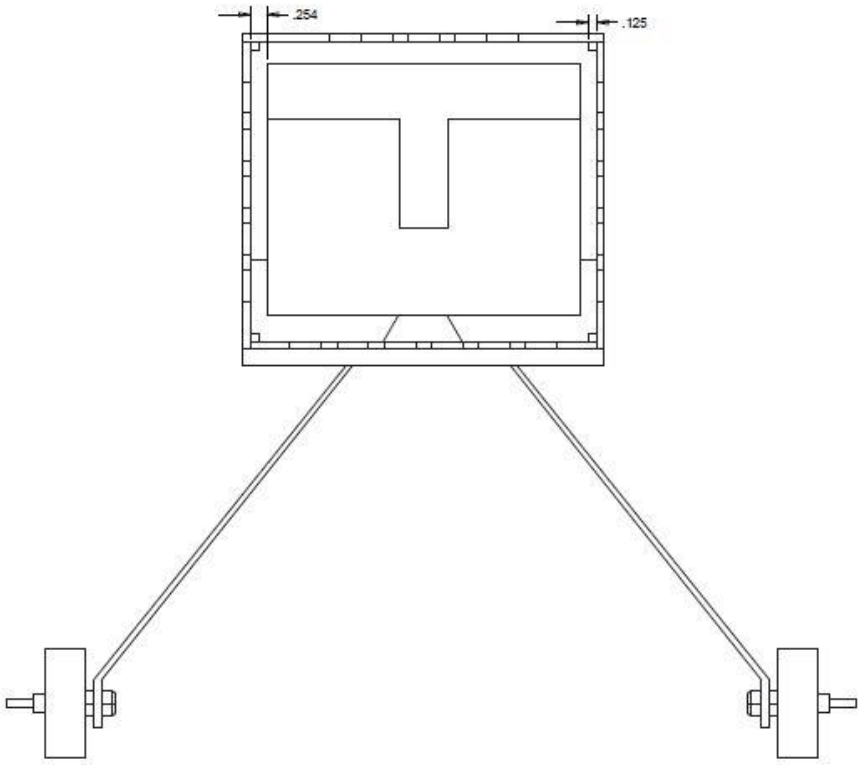

Figure 4. Fuselage Cross Section.

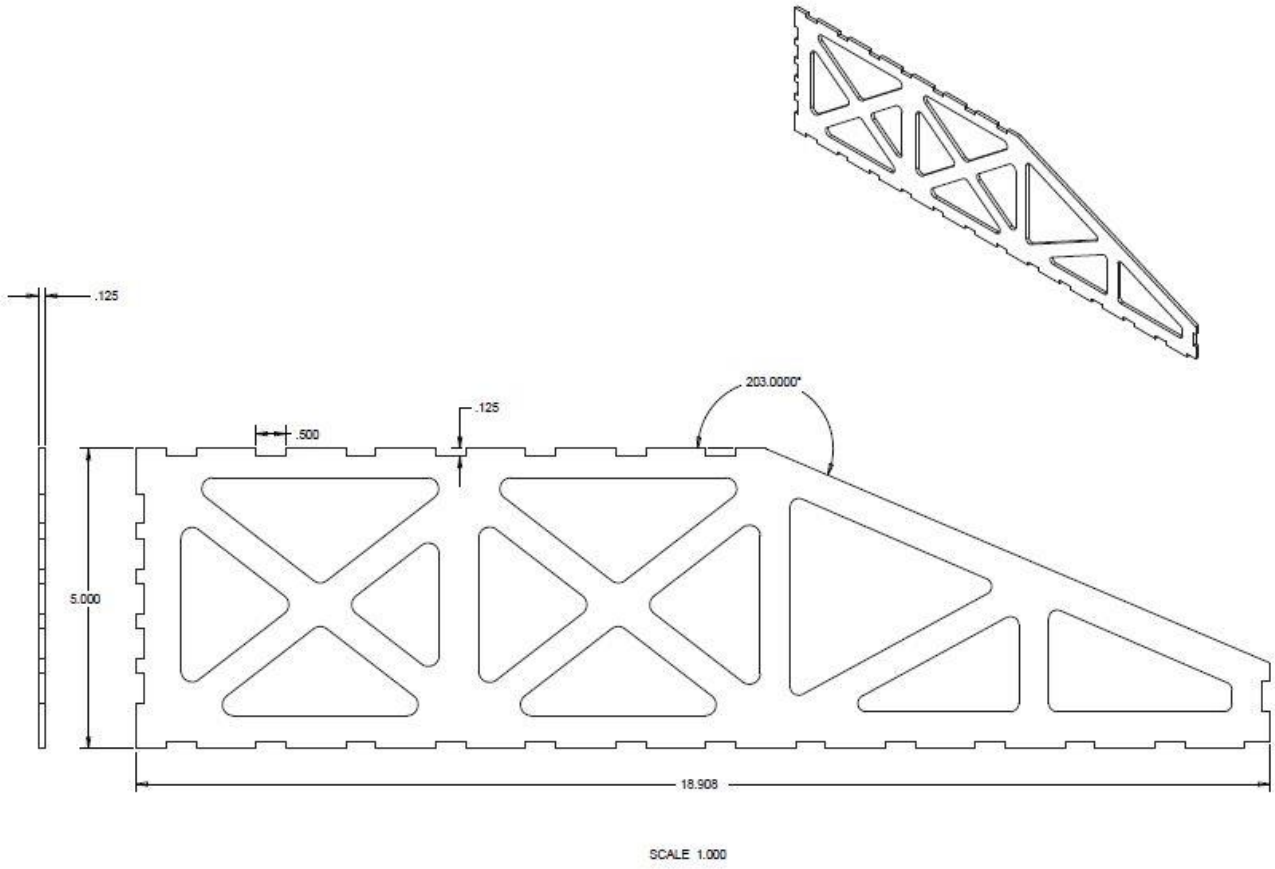

Figure 5. Fuselage Wall.

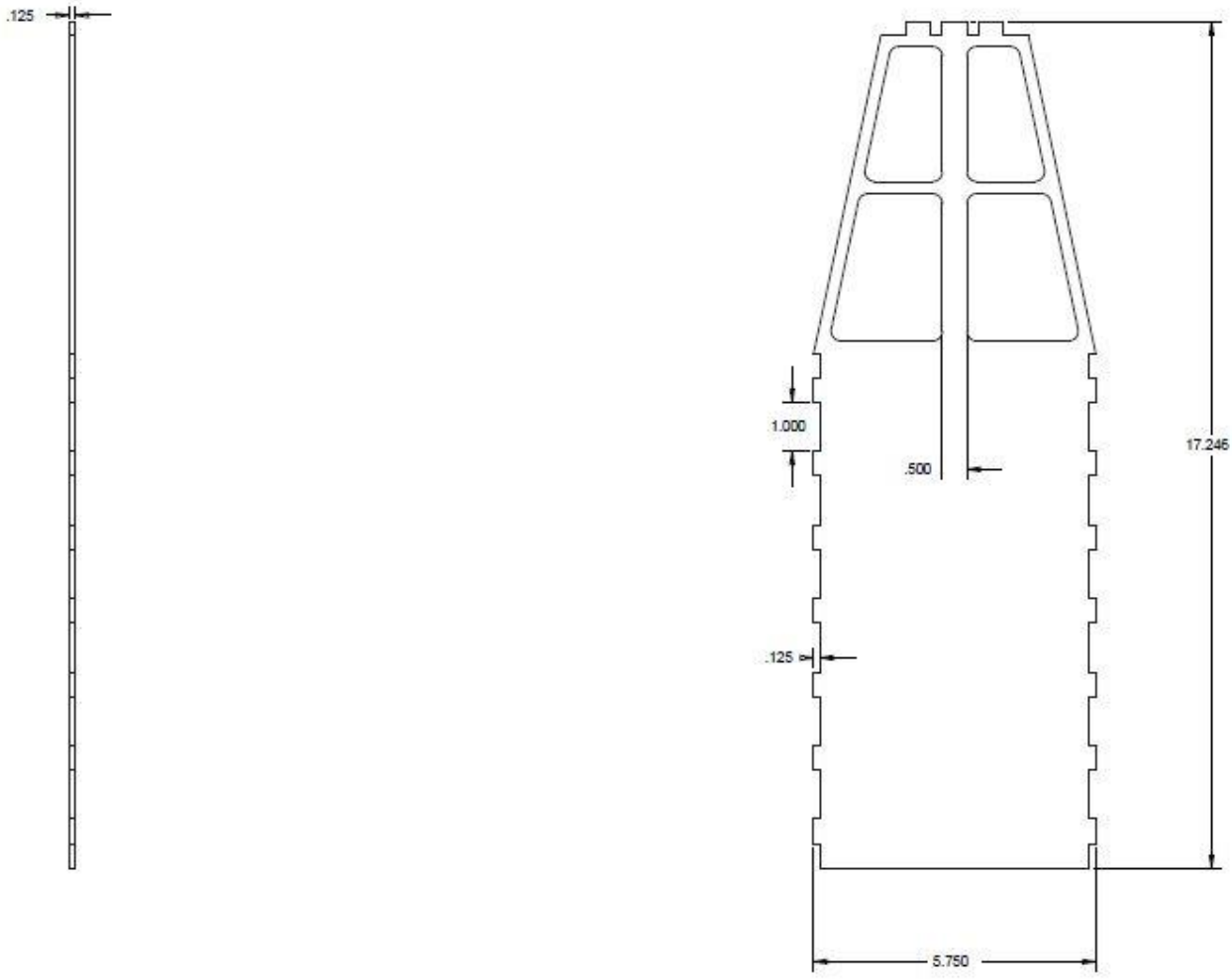

Figure 6. Fuselage Top.

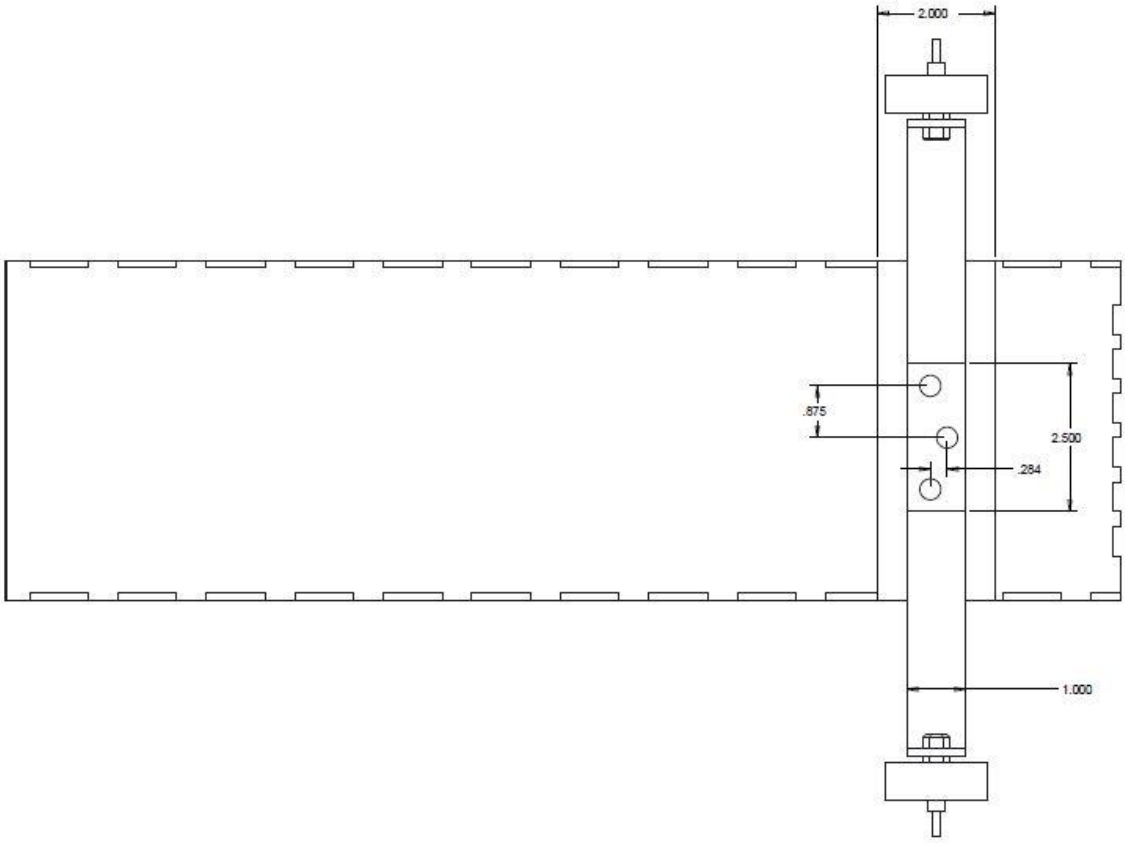

Figure 7. Fuselage Bottom.

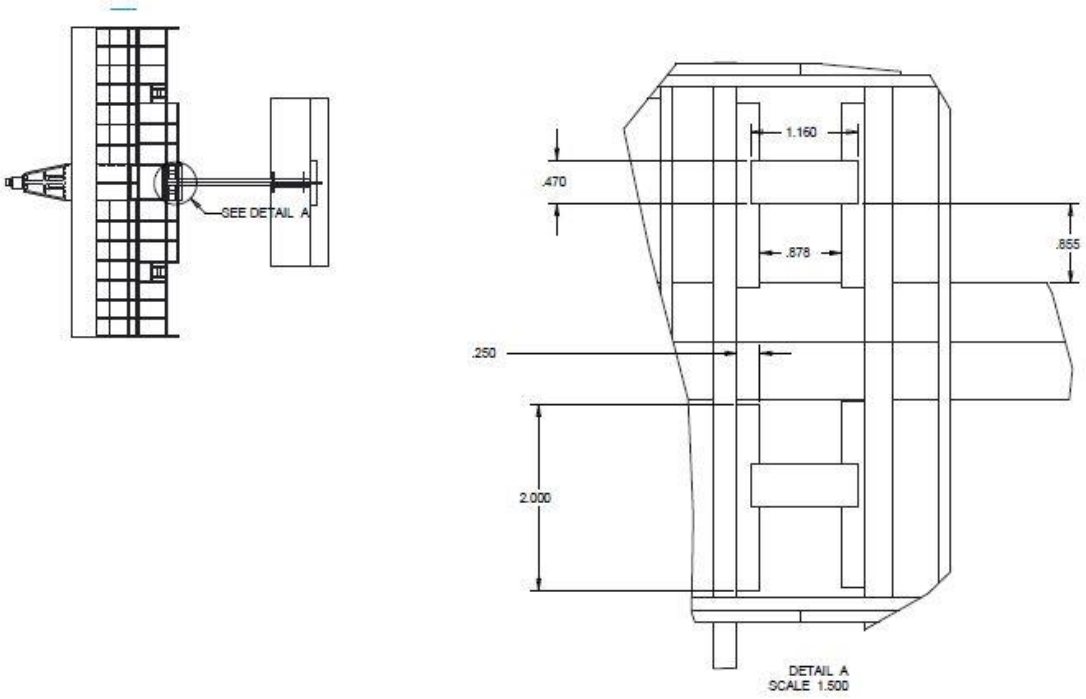

Figure 8. Servo Mount in back of Fuselage.

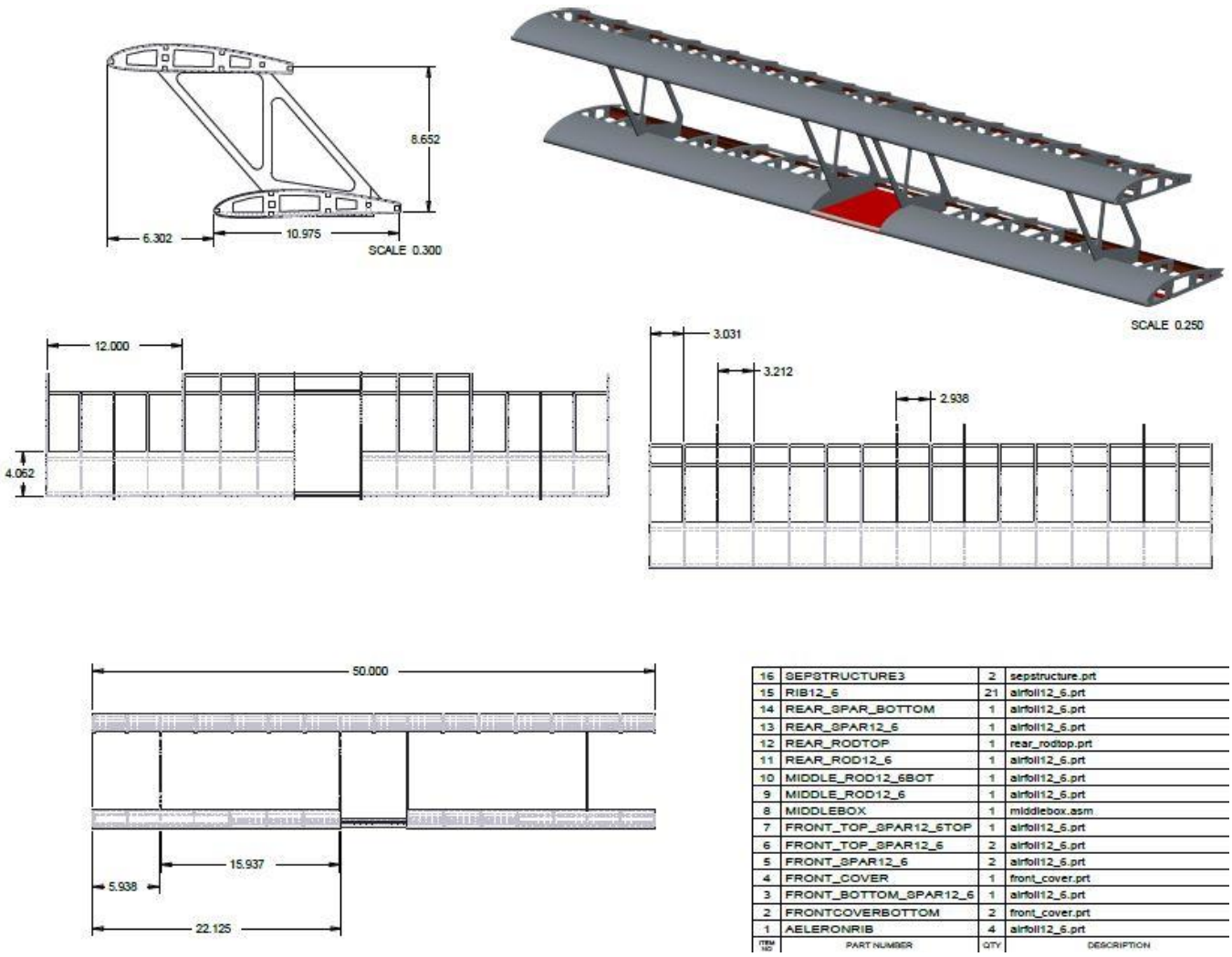

ITEM NO	PART NUMBER	QTY	DESCRIPTION
16	SEPSTRUCTURE3	2	sepstructure.prt
15	RIB12_6	21	airfoil12_6.prt
14	REAR_SPAR_BOTTOM	1	airfoil12_6.prt
13	REAR_SPAR12_6	1	airfoil12_6.prt
12	REAR_RODTOP	1	rear_rodtop.prt
11	REAR_ROD12_6	1	airfoil12_6.prt
10	MIDDLE_ROD12_6BOT	1	airfoil12_6.prt
9	MIDDLE_ROD12_6	1	airfoil12_6.prt
8	MIDDLEBOX	1	middlebox.asm
7	FRONT_TOP_SPAR12_6TOP	1	airfoil12_6.prt
6	FRONT_TOP_SPAR12_6	2	airfoil12_6.prt
5	FRONT_SPAR12_6	2	airfoil12_6.prt
4	FRONT_COVER	1	front_cover.prt
3	FRONT_BOTTOM_SPAR12_6	1	airfoil12_6.prt
2	FRONTCOVERBOTTOM	2	front_cover.prt
1	AELERONRIB	4	airfoil12_6.prt

Figure 9. Wing Detailed Design.

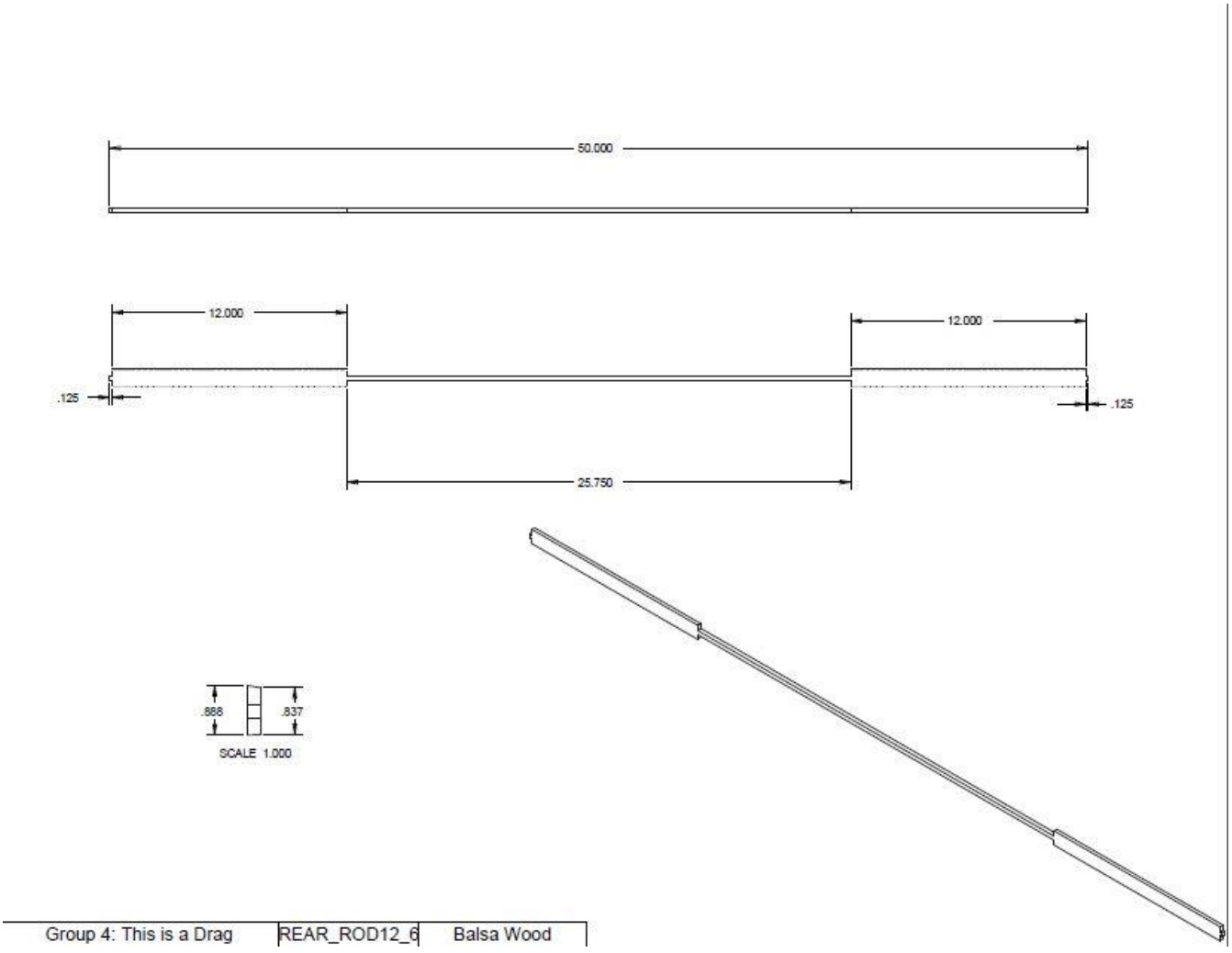

Figure 10. Rear Rod for Wing.

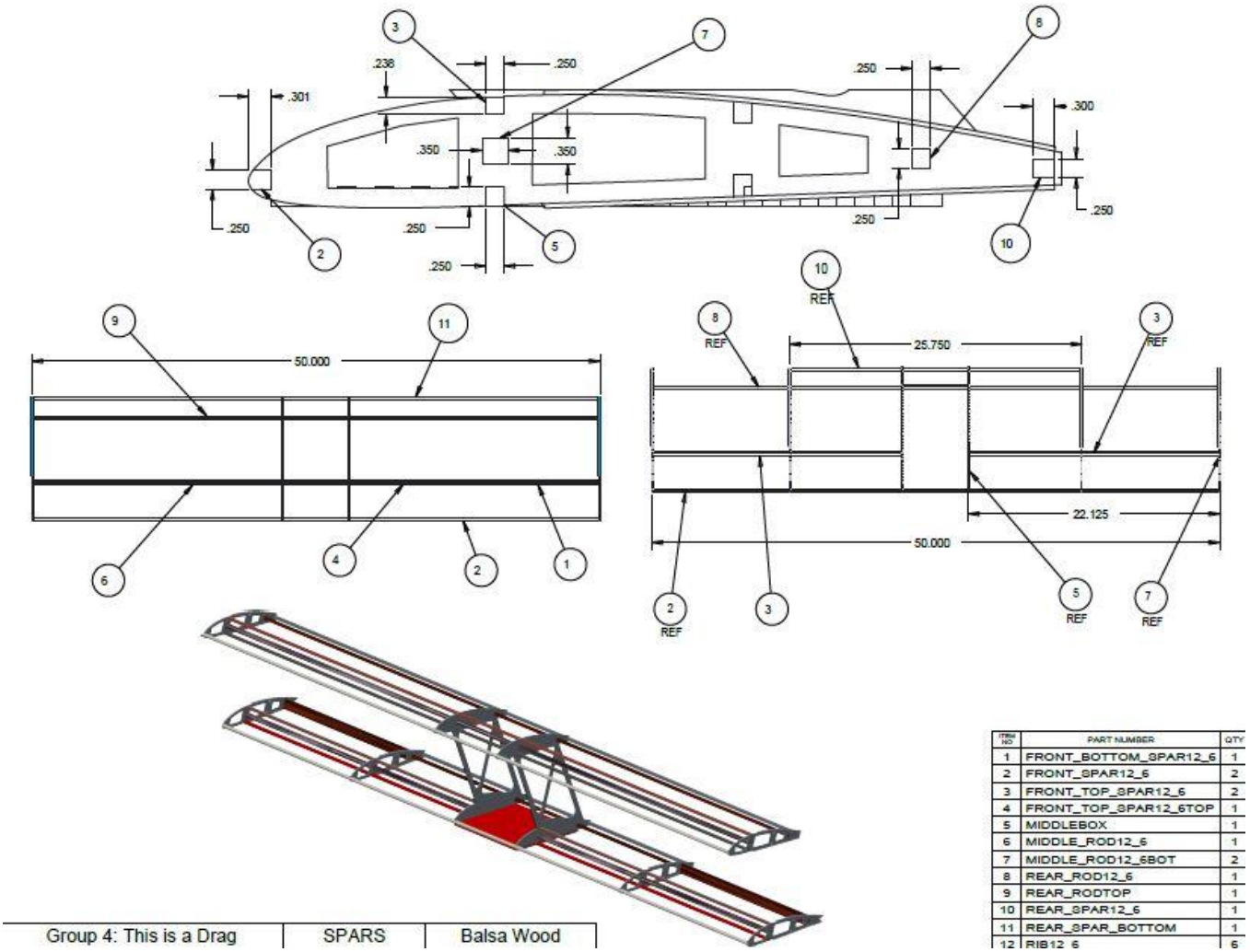

ITEM NO	PART NUMBER	QTY
1	FRONT_BOTTOM_SPAR12_6	1
2	FRONT_SPAR12_6	2
3	FRONT_TOP_SPAR12_6	2
4	FRONT_TOP_SPAR12_6TOP	1
5	MIDDLEBOX	1
6	MIDDLE_ROD12_6	1
7	MIDDLE_ROD12_6BOT	2
8	REAR_ROD12_6	1
9	REAR_RODTOP	1
10	REAR_SPAR12_6	1
11	REAR_SPAR_BOTTOM	1
12	RIB12_6	6

Figure 11. Spars.

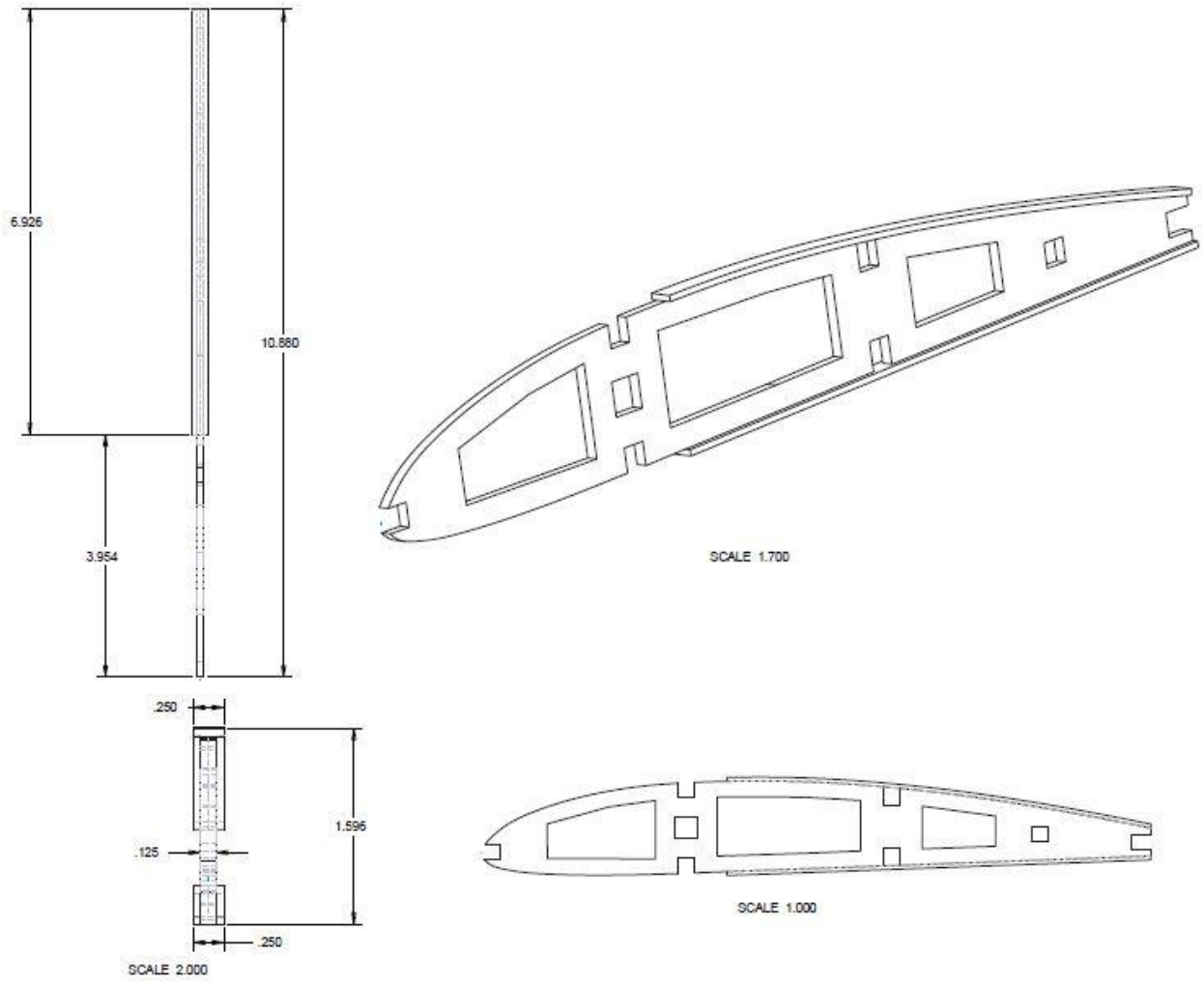

Figure 12. Wing Rib.

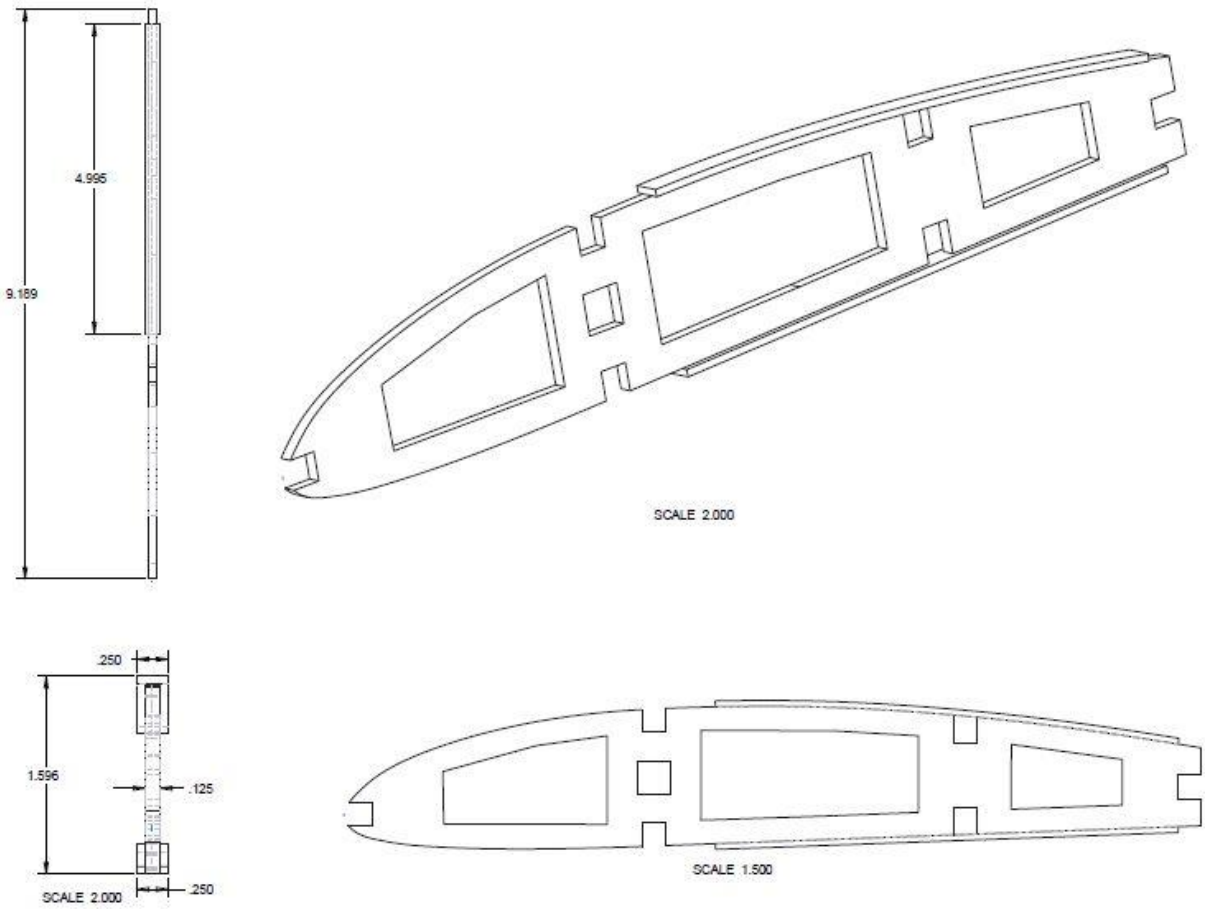

Figure 13. Aileron Rib.

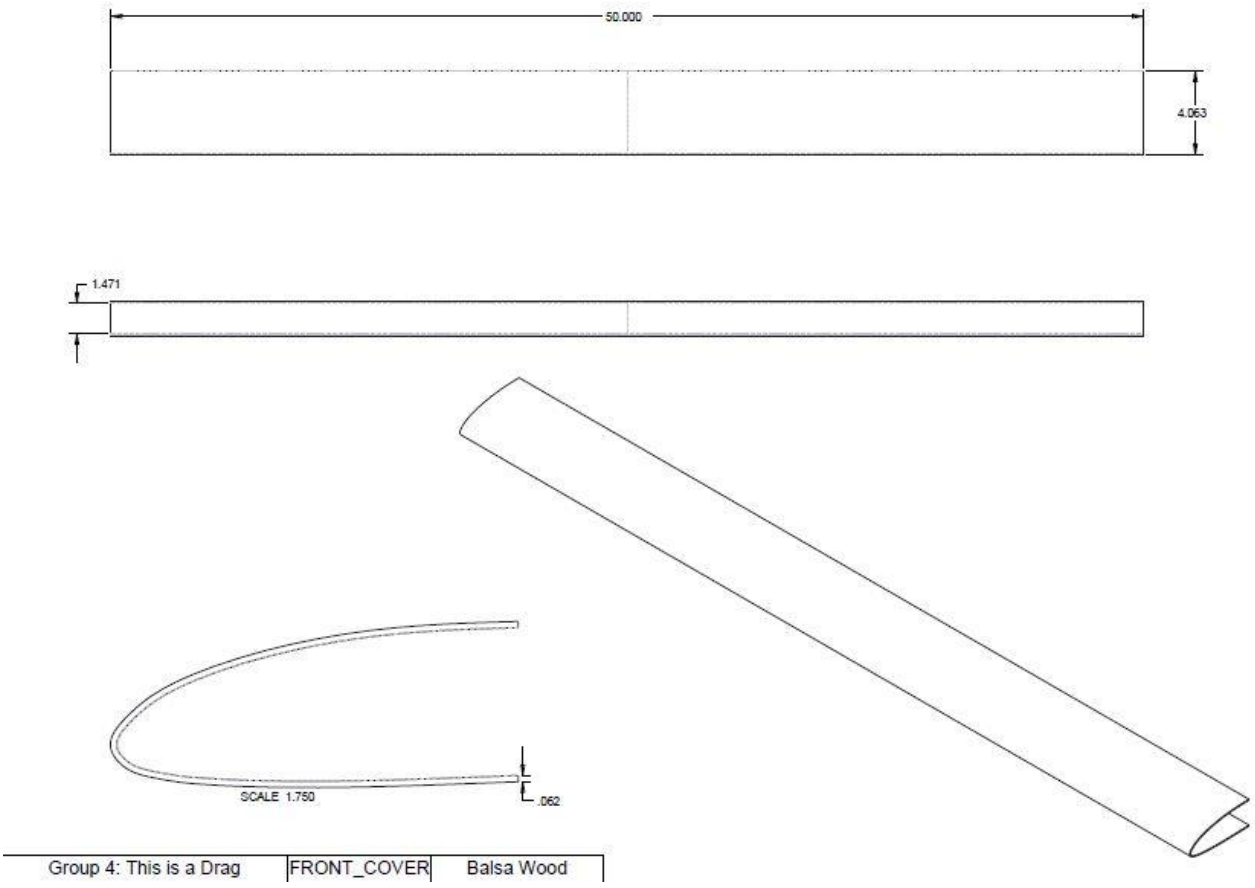

Figure 14. Leading Edge Cover.

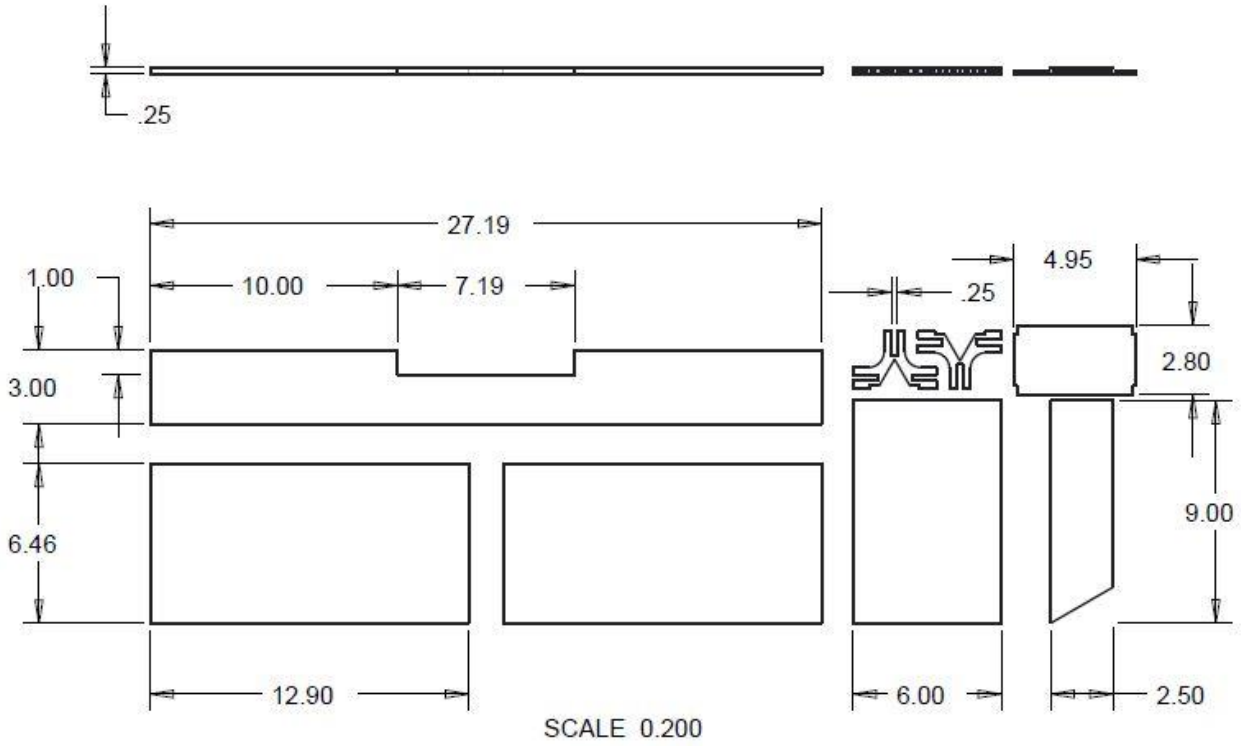

Figure 15. Detailed Tail Pieces.

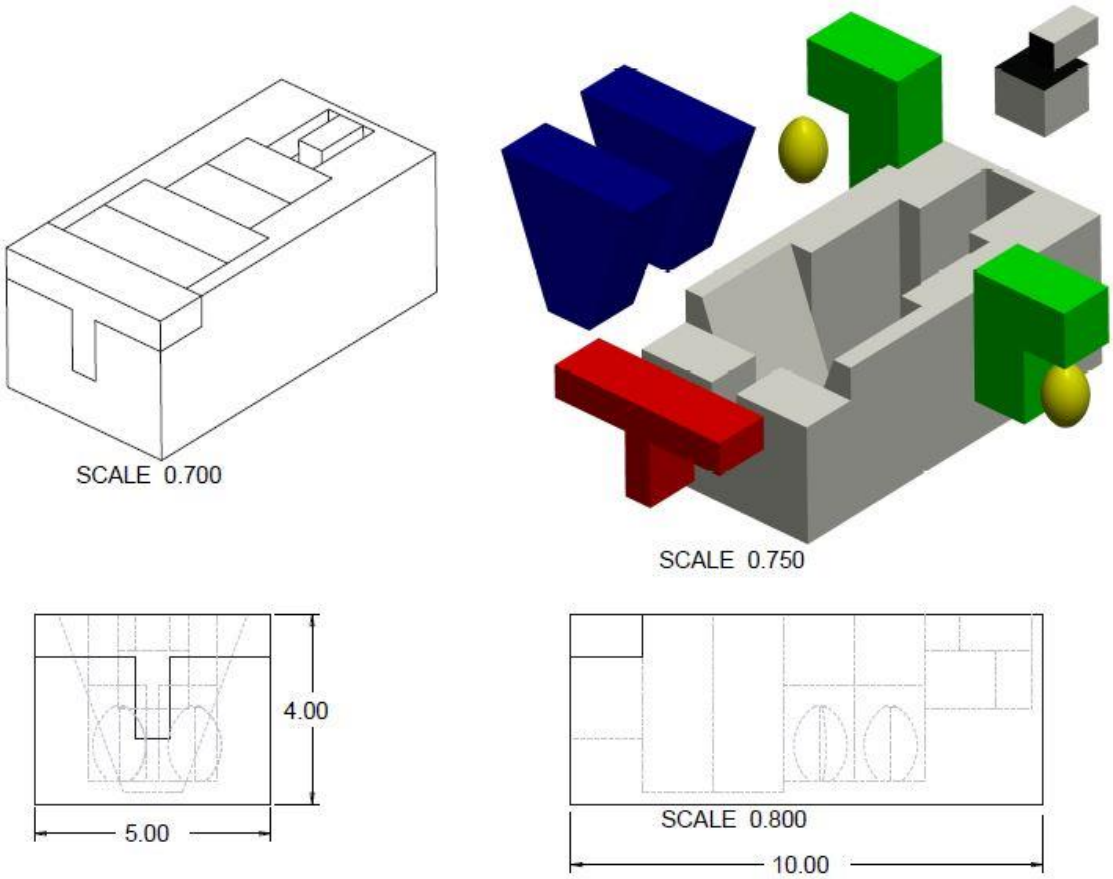

Figure 16. Cargo Tray and Passengers.